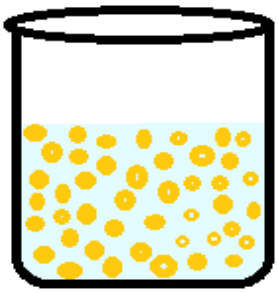

Nanocarriers dispersion

Incorporate into transdermal patch

Nanocarriers + HPMC K4M + PEG 400 + glycerol

Pour in petriplate

Dry in hot air oven

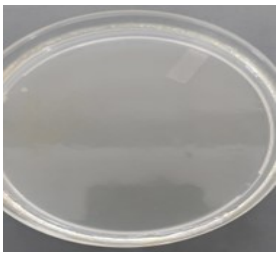

Nanocarriers incorporated transdermal patch

Chapter-9

Nanocarriers incorporated transdermal patch

Evaluation of transdermal patches

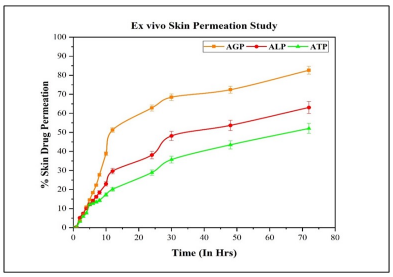

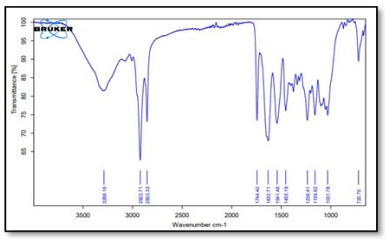

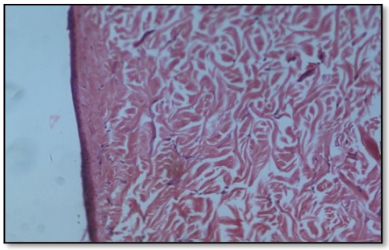

Stability study

9.1. Transdermal Patch:

Transdermal drug delivery systems (TDDS) are self-contained discrete dosage forms that, when applied to normal skin, deliver the drug(s) into the systemic circulation over a prolonged period of time at a predetermined and predictable rate through the skin portal [1, 2]. A transdermal patch, also known as a skin patch, is an adhesive patch applied to the skin that delivers drug that is intended to be absorbed into the bloodstream through the skin [3-6].

9.2. Preparation of transdermal patch:

The transdermal patches were prepared by solvent evaporation method with some modification [2, 7-9]. The polymer was dissolved in suitable solvent with the help of magnetic stirrer. Then, the plasticizer was added in above solution. The resulting solution was then sonicated for complete removal of air bubbles and then poured into petriplate. Then, the solution was allowed to dry in hot air oven for overnight at 35±5°C. After complete drying, the patch was cut into small patches and evaluated for physicochemical characterization.

9.3. Selection of polymer:

Several polymers and their combination were screened for formulation of transdermal patch such as HPMC K4M, HPMC K100M, Ethyl cellulose, polyvinyl alcohol (PVA), etc. The transdermal patches were formulated using different polymers by keeping other parameters constant like drying condition, drying time, concentration of plasticizer etc. The formulated transdermal patch was then evaluated for appearance and physicochemical characteristics.

9.4. Screening and optimization of process and formulation parameters for preparation of transdermal patch:

The various process parameters such as drying time and drying condition, while formulation parameters such as polymer, polymer concentration, plasticizer and its concentration were screened and optimized by using One Factor at A Time (OFAT) technique as described below. The optimization was done on the basis of their physicochemical characteristics such as appearance, weight, thickness, folding endurance, tensile strength, moisture content and moisture uptake.

Table- 9.1. Process and formulation variables studied for transdermal patch development

Variables		Screened values/levels	
Process variables	Drying condition	Room temperature	35±5°C in hot air oven
	Drying time (Hr)	18±0.5	30±0.5
Formulation variables	Polymer concentration (%)	0.5	3.0
	Plasticizer	PEG-400, dibutyl phthalate and propylene glycol	
	Plasticizer concentration (%)	0	10

9.5. Incorporation of glycerosomes into transdermal patch:

HPMC K4M as a polymer and Polyethylene glycol-400 as a plasticizer was added in drug loaded glycerosomal dispersion and mixed at 1000 rpm for 15 min. The mixture was then sonicated to remove air bubbles and poured into a petri-plate with known dimensions and allowed to dry for 24 hours at 35±5°C. After drying, the formed patch was carefully removed. The patch was cut into small patches and evaluated for physicochemical characteristics [2, 7-9].

9.5.1. Incorporation of PECN into transdermal patch:

HPMC K4M as a polymer, polyethylene glycol-400 as a plasticizer and glycerol was added in drug loaded PECN and mixed at 1000 rpm for 15 min. The mixture was then sonicated to remove air bubbles and poured into petri-plate of known dimension and allowed to dry at 35±5°C for 24 hrs. After drying, the formed patch was removed carefully. The patch was cut into small patches containing equal amount of drug [2, 7-9].

9.5.1.1. Selection and optimization of penetration enhancer:

The polyelectrolyte complex nanoparticles showed slower diffusion of drug through skin as reported earlier in ex vivo skin permeation study (in chapter- 7 and 8). The addition of a penetration enhancer (PE) might help to improve the drug penetration through skin layers. Hence, penetration enhancers were added in the preparation of the transdermal patch containing drug-loaded PECN. Different penetration

enhancers like olive oil, glycerol, oleic acid, IPM and propylene glycol in concentration of 0.2% w/w were studied.

The drug loaded PECN with permeation enhancer incorporated transdermal patch were subjected to ex vivo skin permeation study by Franz diffusion cell using rat skin. The skin was sandwiched between donor and receptor compartment. The patch was placed in the donor compartment and receptor compartment was filled with PBS 7.4 (in case of ATO loaded PECN, receptor compartment filled with PBS 7.4 containing 2% propylene glycol). After 24 hrs, the sample was collected from the receptor medium and analyzed by HPLC method.

9.5.1.2. Optimization of concentration of permeation enhancer:

After the selection of permeation enhancer, its concentration was varied from 0.1 to 0.3 % w/w and the prepared patches were then evaluated for their physicochemical characteristics. The optimization of permeation enhancer was done based on maximum amount of drug permeated through skin. The prepared transdermal patch was subjected to an ex vivo skin permeation study as per the procedure mentioned above (in 9.6.1.1. section).

9.6. Physicochemical characteristics of transdermal patch:

9.6.1. Physical Attributes:

The transdermal patches were assessed for morphological parameters like color, clarity, and surface texture [10].

a. Weight variation and thickness:

The prepared transdermal patches of same dimensions were evaluated for uniformity in weight by using digital electronic weighing balance (Type AX 120 and ELB 300, Shimadzu, Japan) [9]. The thickness of transdermal patch was evaluated by using thickness tester (Model No.-2046, Mitutoyo, Japan) [11]. The thickness of patch was measured from three different points and result represented in average [10, 12].

b. Folding endurance:

The folding endurance of a transdermal patch was measured by repeatedly folding the patch at the same place until it broke. The number of times the film could be folded at the same place without breaking gives folding endurance value [2, 10, 13, 14].

9.6.2. Percentage moisture uptake and moisture content:

The prepared patches were cut (2 X 2 cm) and accurately weighed. Then, these patches were kept in desiccator containing calcium chloride at room temperature for 24 hrs. After 24 hrs, each patch was reweighed separately. The moisture content of patch was calculated by using following equation [2, 14-16]:

$$Moisture\ Content\ (\%) = \frac{Initial\ weight - Final\ weight}{Final\ weight} \times 100$$

……..equation- 9.1.

The moisture uptake capacities of patch were measured at 84 % RH (in a saturated solution of aluminium chloride). The patches were cut (2 X 2 cm) and accurately weighed at predetermined time interval until constant weight. The moisture uptake was calculated by following equation [2, 14-16]:

$$Moisture\ Uptake\ (\%) = \frac{Final\ weight - Initial\ weight}{Initial\ weight} \times 100$$

……..equation- 9.2.

9.6.3. Tensile strength:

The tensile strength of patch was determined by digital tensiometer (Brookfield texture analyzer; Brookfield, IL, USA) by clamping the patch of specific dimension (2 X 2 cm) and elongating by instrument till it deformed. The force and distance travelled was calculated and graph was generated [9, 13, 17, 18].

$$Tensile\ strength = \frac{Breaking\ force\ (g)}{Cross\ sectional\ area\ of\ film\ (cm^2)}$$

……..equation- 9.3.

9.6.4. Drug content:

The patch of size of 2 X 2 cm was cut from three different places, dissolved in 50 ml of 50% methanolic aqueous solution and stirred for 2 hrs on magnetic stirrer at 1000 rpm. The appropriate dilution was made and analyzed by UV spectrophotometer against blank (UV -1900, Shimadzu, Japan) [1, 10, 18, 19].

9.7. *Ex vivo* skin permeation and deposition study:

a. Skin collection and preservation:

The Skin collection and preservation is described in chapter 5 (in *Ex vivo* skin permeation study section).

b. Experimental procedure:

The experimental procedure for ex vivo skin permeation study is described in section 9.6.1.1. After completion of the permeation study, the skin was removed from the Franz diffusion cell, and the donor side was washed with PBS. The washed sample was collected for calculation of how much drug remained on the skin. The skin was then cut into small pieces and suspended into methanol. The suspension was homogenized for 15 min and sonicated using bath sonicator to extract drug which was accumulated into skin layers. After that, the samples were centrifuged for 10 minutes at 5000 rpm. The supernatant was collected and filtered through 0.45 µm syringe filter and analyzed [20-23].

The permeation enhancement ratio were calculated as follows [24]:

$$Permeation\ enhancement\ ratio\ = \frac{J_{ss}\ Test}{J_{ss}\ Control}$$

…….equation- 9.4.

9.8. Evaluation of skin structure by FTIR study:

In order to understand the impact of the drug and excipients used in the formulation on the skin structure, Fourier transform infrared spectroscopy was used to assess the integrity of the skin structure following the application of the formulation [25].

The procedure for skin collection and preservation is same as ex vivo skin permeation study. The skin was mounted between donor and receptor compartment of Franz diffusion cell. The transdermal patch was applied on the skin for 24 hrs. After 24 hrs, the skin was washed with phosphate buffer pH 7.4 and dried at room temperature for 24 hrs. After drying, the skin sample was analysed by FTIR spectrophotometer [25-27]. The untreated skin was used as a control and compared with drug loaded nanocarriers incorporated transdermal patch treated skin.

Control sample: Untreated skin (Normal skin)

Test samples: Skin treated with

(1) ATO loaded glycerosomal transdermal patch

(2) RSNa loaded glycerosomal transdermal patch

(3) ATO-PECN loaded transdermal patch

(4) RSNa-PECN loaded transdermal patch

9.9.*Ex vivo* skin permeation analysis by using fluorescence microscopy:

The procedure of skin collection is same as ex vivo skin permeation study described earlier. The skin was mounted in between donor and receptor compartment of Franz diffusion cell. The transdermal patch was placed on skin for 24 hrs. After 24 hr treatment, the skin was washed with phosphate buffer and fixed into 10% formaldehyde. The skin was hydrated and embedded in paraffin. The samples were sectioned to 10 µm thickness. The collected sectioned were examined by fluorescence microscope. The treated skin was compared with untreated skin (normal control) [25, 26, 28].

Fluorescence dyes: Fluorescein isothiocyanate (FITC) and Rhodamine B

Filter used in microscope: 1. Fluorescein isothiocyanate for green filter (400–530 nm nanometers).

2. Tetramethylrhodamine isothiocyanate for red filter (excitation peak at 544 nm and an emission peak at 570 nm).

Test samples: (1) Untreated skin

(2) ATO loaded glycerosomal transdermal patch

(3) RSNa loaded glycerosomal transdermal patch

(4) ATO-PECN loaded transdermal patch

(5) RSNa-PECN loaded transdermal patch

9.10. Histopathological studies:

The objective of the histological investigation was to determine the changes that occur on the skin after treatment of transdermal patch [28].

The procedure for collection and preservation of skin specimen was same as described in ex vivo skin permeation study. The skin was mounted in between donor and receptor compartment of Franz diffusion cell. The transdermal patch was placed on skin for 72 hrs. After 72 hrs, the skin was washed with phosphate buffer and fixed with 10% formaldehyde. The skin was hydrated and eventually entrenched in paraffin. The skin was sliced to section of 10 µm thickness. The sliced section was stained with hematoxylin and eosin (H&E). The collected section was examined by inverted microscope (Nikon Ti2E, USA). The abnormalities (edema) after treatment of transdermal patch were observed and compared with normal (untreated) skin [25, 28-30].

9.11. Stability study:

Stability studies were performed on nanocarriers loaded transdermal patch in accordance with the standards of the International Conference on Harmonization. The stability studies were carried out by putting the transdermal patch for 3 months at three different storage condition viz. at 2-8 °C, 25±2°C /65±5% RH and 40±2°C /75±5% RH in stability

chamber [1, 26, 31]. At intervals of 30 days, the patches were tested for morphology, drug content, weight variation, thickness, and folding endurance. All tests were analyzed in triplicate and compared with initial results.

9.12. Results and discussion:

Transdermal patch – Formulation development

The present work covers the formulation development of transdermal patch incorporated with nanocarriers. The screening and optimization of process and formulation were carried out by OFAT technique to check the effect of variables on different responses such as appearance, tensile strength, weight, thickness, folding endurance, % moisture uptake and % moisture content. After optimization of placebo transdermal patch, the nanocarriers were incorporated.

9.13. Selection of polymers for transdermal patch preparation:

Several patches were prepared using different polymers such as HPMC K4M, HPMC K100M, HPMCK15M, Polyvinyl alcohol (PVA) and combination of PVA with different grades of HPMC. Based on the results of the study (shown in table-9.2), the patch prepared using PVA was smooth and translucent, but brittle and was unable to be easily peeled out of the petriplate. The patch prepared from a mixture of HPMC K4M and ethyl cellulose appeared hazy, thick, and brittle.

The patches prepared with combination of HPMC K4M and PVA were found to be smooth and transparent in nature. The prepared patches showed weight in range of 162 to 242 mg and thickness in between 0.41 to 0.49 mm which was more than weight of patch prepared using alone HPMC due to presence of moisture in the patch. The patches showed lower folding endurance and tensile strength as compared to alone HPMC prepared patches. % moisture content and % moisture uptake were high due to the hydrophilic nature of HPMC and PVA [32].

The patches prepared using different grades of HPMC such as K4M, K15M and K100M were smooth and transparent in appearance. Their tensile strength and folding endurance were found to be higher than other patches. The low moisture content and moisture uptake indicated that the patches will remain stable during long term storage.

Table- 9.2. Selection of polymer for preparation of transdermal patch

Polymer	Observations						
	Appearance	**Weight (mg)**	**Thickness (µm)**	**Folding endurance**	**Tensile strength (gm/cm^2)**	**% moisture content**	**% moisture uptake**
HPMC K4 M	Smooth and transparent	141.7 ± 2.51	0.40 ± 0.005	390 ± 5.03	871.25 ± 24.87	1.03 ± 0.58	1.38 ± 0.64
HPMC K 15 M	Smooth and transparent	148.9 ± 2.89	0.40 ± 0.01	338 ± 3.06	531.75 ± 50.23	3.63 ± 1.11	6.42 ± 2.12
HPMC K 100 M	Smooth and transparent	152.2 ± 3.33	0.41± 0.01	297 ± 5.56	466.00 ± 38.12	7.11 ± 1.37	9.47 ± 2.53
PVA	Smooth and transparent but Brittle film was formed.						
HPMC K 4M + Ethyl Cellulose	Hazy, brittle, and thick film was formed.						
HPMC K4M + PVA	Smooth and transparent	167.8 ± 3.56	0.41 ± 0.00	215 ± 4.04	301.50 ± 18.12	5.91 ± 1.20	3.72 ± 0.83
HPMC K100M + PVA	Smooth and transparent	178.2 ± 3.15	0.48 ± 0.01	186 ± 6.80	228.25 ± 15.78	4.73 ± 1.93	2.96 ± 0.74
HPMC K15M + PVA	Smooth and transparent	242.4 ± 2.12	0.49 ± 0.01	251 ± 5.00	432.00 ± 21.93	3.69 ± 1.21	2.36 ± 0.98

(n=3, ± S.D.)

Among these patches, the patches prepared using HPMC K4M were smooth and transparent with maximum tensile strength and folding endurance and showed low moisture content and moisture uptake. Hence, on the basis of overall results, HPMC K4M was selected as the polymer for further development of the transdermal patch.

9.14. Screening and optimization of process and formulation parameters:

9.14.1. Screening and optimization of process parameters for transdermal patch:

The process parameters for preparation of transdermal patch such as drying condition and drying time were screened and optimized as follows:

9.14.1.1. Selection of drying condition:

At 35±5°C drying conditions, better peeling of the transdermal patch from petri plates with good physicochemical characteristics was observed. The transdermal patch dried at 35±5 °C had minimum percentage of moisture content, which indicated complete evaporation of solvent from the patch. Hence, drying condition at 35±5°C (in hot air oven) was selected as optimum for further development.

9.14.1.2. Selection of drying time:

In order to make a good and stable transdermal patch, it was important to know how long it would take for the patch to dry completely. There was sufficient time of 24 hrs to completely dry the transdermal patch with a minimum % moisture content and high folding endurance and tensile strength. The patch was broken and not properly peeled out of the petri plates after 30 hours, possibly due to excessive drying. In 18 hours of drying time, the evaporation of solvent did not take place completely, resulting in the formation of an improper patch. Hence, 24 hours of drying time was selected as the optimum for further development.

Table- 9.3. Effect of process parameters on preparation of transdermal patch

Selection of drying condition		
Selection of drying condition	**Observations**	
	At room temperature	**At 35±5°C**
Appearance	Smooth and Transparent	Smooth and Transparent
Weight (mg)	203.7 ± 4.32	148.1 ± 2.15
Thickness (mm)	0.42 ± 0.005	0.40 ± 0.01
Folding endurance	105 ± 9.29	376 ± 8.00
Tensile strength (gm/cm^2)	205.5 ± 21.56	928.0 ± 32.51
% moisture content	10.58 ± 2.21	1.13 ± 0.69
% moisture uptake	4.57 ± 1.34	1.85 ± 0.41

Selection of drying time			
Selection of drying time	**Observations**		
	18 ± 0.5 hrs	**24 ± 0.5 hrs**	**30 ± 0.5 hrs**
Appearance	Smooth and Transparent	Smooth and Transparent	Smooth and Transparent
Weight (mg)	165.1 ± 4.33	150.3 ± 3.20	145.8 ± 2.23
Thickness (µm)	0.42 ± 0.01	0.40 ± 0.005	0.39 ± 0.005
Folding endurance	200 ± 4.52	389 ± 5.18	28 ± 5.00
Tensile strength (gm/cm^2)	636.2 ± 18.32	911.5 ± 36.18	219.1l ± 21.55
% moisture content	8.78 ± 2.12	3.15 ± 1.02	2.90 ± 1.26
% moisture uptake	4.36 ± 1.68	2.08 ± 0.81	2.16 ± 0.98

(n=3, ± S.D.)

9.14.2. Screening and optimization of formulation parameters for transdermal patch:

The formulation parameters such as polymer concentration, selection of plasticizer and its concentration were screened and optimized by OFAT as follows:

9.14.2.1. Screening and optimization of HPMC K4M concentration:

The polymer concentration was varied from 0.5% to 3% and effect of concentration on physicochemical parameters were evaluated. From the results (table- 9.4), it was observed that increase in the concentration of polymer slightly increased the weight and thickness of patch. The moisture content and moisture uptake were increased with increase in concentration of HPMC K4M might be due to hydrophilic nature of polymer that had capacity of absorption of water molecules [33]. Tensile strength was affected by polymer concentration, and this could be attributed to the excellent film forming properties of polymer [34]. The folding endurance and tensile strength were increased with increase in concentration of HPMC K4M [34, 35], giving the patch increased rigidity with good physical stability [36]. The more folding endurance indicates the film will retain its form and integrity throughout application [17]. The more tensile strength value indicated that the film would be flexible and facilitate good stretching during movement of body parts after application [17]. From the results, it was concluded that 2 % concentration of HPMC K4M showed good physicochemical and mechanical properties. When the concentration was increased above 2%, there was no noticeable difference observed in physicochemical characteristics. Hence, 2 % w/w concentration of HPMC K4M was selected as optimum for further development.

9.14.2.2. Selection of plasticizer:

Plasticizer is an important component in determining the elastic properties of a patch [37]. To withstand external factors such as wear and tear during handling, storage, or usage, patches should be elastic in nature [37-39]. Plasticizers reduce polymer-polymer chain secondary bonding and instead produce secondary bonds with the polymer chains [34]. Plasticizers are used in transdermal medication delivery systems to enhance film forming capabilities and the appearance of the film. The effect of different plasticizer on physicochemical characteristics of patch are shown in table- 9.4. From the results, it was observed that PEG-400 showed better folding endurance, tensile strength, % moisture content and % moisture uptake than dibutyl phthalate and propylene glycol. The tensile strength of hydrophilic plasticizers was higher than that of hydrophobic plasticizers. These

results were rendered possible due to the hydrophilic-hydrophobic interactions of polymers and plasticizers, in which hydrophobic plasticizers disrupt the miscibility of polymer chains, resulting in lower tensile strength [35]. The moisture content and moisture uptake of propylene glycol and PEG-400 was more than dibutyl phthalate due to their humectant property. Moreover, the patches formulated with PEG 400 showed significantly lower moisture content as compared to PG, suggesting that the plasticizer will assist the formulation to remain stable and less brittle during long-term storage, particularly in dry conditions [40]. Hence, PEG-400 was selected as plasticizer for further development.

9.14.2.3. PEG-400 concentration:

The results of screening and optimization of PEG-400 concentration are represented in table- 9.4. The folding endurance measures the film's capacity to withstand rupture when applied to the skin surface [16]. The results showed that increase in concentration of PEG-400 increased folding endurance upto certain level because plasticizers relax the hydrogen bonds that exist between polymers, resulting in increased folding endurance [41]. When the concentration of PEG exceeds 5%, the folding endurance decreases, possibly due to a loss of the polymeric network. Increase in concentration of PEG upto 5%, increased the tensile strength of patch due to high polymer cross-linking structures that increase elongation ability and reduce polymer fragility by plasticizer [34]. When the concentration of PEG-400 exceed 5 %, the tensile strength decreases with increase in PEG concentration might be due to plasticizer molecules may break polymer interchain cohesive forces [39]. The results implies that the prepared patches have adequate tensile strength, flexibility, can tolerate mechanical pressure, and can keep integrity with general skin folding when applied [16]. There was no significant difference observed on thickness of patch after increase in concentration of PEG. The slight increase in weight was observed with increase in concentration of PEG. The increase in concentration of PEG increased % moisture content and uptake might be due hydrophilic nature of PEG which provides ability to absorb water molecule [1]. On the basis of overall results, 5% w/w PEG-400 was selected as optimum for further development.

Table- 9.4. Effect of formulation parameters on preparation of transdermal patch

HPMC K4M concentration (%)				
Polymer concentration	**Observations**			
	0.5	**1**	**2**	**3**
Appearance	Smooth and Transparent	Smooth and Transparent	Smooth and Transparent	Smooth and Transparent
Weight (mg)	118.2 ± 3.50	133.5 ± 3.85	145.1 ± 2.15	172.8 ± 3.63
Thickness (µm)	0.39 ± 0.01	0.40 ± 0.005	0.42 ± 0.005	0.46 ± 0.01
Folding endurance	214 ± 14.52	276 ± 9.50	389 ± 7.51	354 ± 6.11
Tensile strength (gm/cm^2)	546.0 ± 30.21	665.25 ± 24.18	885.25 ± 28.48	909.25 ± 51.25
% moisture content	1.28 ± 0.76	1.98 ± 0.82	1.82 ± 0.64	3.87 ± 1.26
% moisture uptake	1.02 ± 0.37	1.69 ± 0.55	1.18 ± 0.37	4.19 ± 0.78
Plasticizer selection				
Plasticizer	**Observations**			
	PEG-400	**Dibutyl phthalate**	**Propylene glycol**	
Appearance	Smooth and Transparent	Smooth and Transparent	Smooth and Transparent	
Weight (mg)	143.3 ± 3.45	156.2 ± 4.18	150.8 ± 3.68	
Thickness (µm)	0.40 ± 0.005	0.40 ± 0.01	0.41 ± 0.01	
Folding endurance	398 ± 4.00	218 ± 8.73	315 ± 5.56	
Tensile strength (gm/cm^2)	865.75 ± 28.96	726.5 ± 39.62	756.6 ± 36.52	
% moisture content	0.85 ± 0.48	1.71 ± 1.21	1.96 ± 0.97	
% moisture uptake	1.56 ± 0.46	1.84 ± 0.90	2.09 ± 0.55	

Plasticizer concentration	PEG-400 concentration (%) Observations				
	0	**2.5**	**5**	**7.5**	**10**
Appearance	Smooth and Transparent	Smooth and Transparent	Smooth and Transparent	Smooth and Transparent	Smooth and Transparent
Weight (mg)	132.5 ± 3.36	140.1 ± 3.84	142.7 ± 2.85	148.3 ± 2.62	158.8 ± 3.65
Thickness (µm)	0.38 ± 0.005	0.39 ± 0.01	0.40 ± 0.01	0.40 ± 0.01	0.42 ± 0.01
Folding endurance	178 ± 9.01	266 ± 7.02	392 ± 4.50	325 ± 7.00	292 ± 4.16
Tensile strength (gm/cm^2)	229.5 ± 14.36	616.25 ± 16.85	903.0 ± 18.15	861.0 ± 29.87	801.3 ± 25.17
% moisture content	3.88 ± 0.89	1.63 ± 0.75	1.03 ± 0.65	1.36 ± 0.81	1.48 ± 0.61
% moisture uptake	1.65 ± 0.57	0.90 ± 0.43	1.12 ± 0.38	1.98 ± 0.47	2.52 ± 1.01

(n=3, ± S.D.)

The optimized process and formulation parameters for formulation of transdermal patch are shown in table- 9.5.

Table- 9.5. Optimized process and formulation parameters for transdermal patch

Parameters	Optimum values
Concentration of HPMC K4M (% w/w)	2
Plasticizer	PEG-400
PEG-400 concentration (% w/w)	5
Drying condition	At 35±5°C (in hot air oven)
Drying time (hrs)	24 ± 0.5

The above optimized process and formulation parameters were used for further development of transdermal patch.

9.15. Incorporation of nanocarriers into transdermal patches:

The drug loaded nanocarriers were incorporated into transdermal patches using above optimized parameters (shown in table- 9.5) and evaluated for different physicochemical characteristics such as drug content, appearance, weight, thickness, folding endurance, tensile strength, % moisture content and % moisture uptake as well as different ex vivo studies such as skin permeation, FTIR of treated skin, histopathology, fluorescence microscopic study and stability study.

9.15.1. Glycerosomes incorporated transdermal patches:

9.15.1.1. ATO loaded glycerosomal transdermal patch - Formulation development

The optimized ATO loaded glycerosomes containing different concentration of glycerol i.e., 0% w/w and 30% w/w (shown in chapter 5) were incorporated into above optimized transdermal patch and evaluated. The control transdermal patch was prepared by incorporating ATO (in equivalent amount to ATO loaded glycerosomes) instead of glycerosomes by using same method. The results of ATO loaded glycerosomal transdermal patch and ATO loaded transdermal patch are shown in table- 9.6.

Table- 9.6. Physicochemical characteristics of ATO loaded glycerosomal transdermal patches

PARAMETERS	VALUES		
	0 % w/w* (ALP)	30 % w/w* (AGP)	ATO Loaded Patch (ATP)
Appearance	Smooth and Translucent	Smooth and Translucent	Smooth and Transparent
Thickness (mm)	0.38 ± 0.005	0.40 ± 0.011	0.34 ± 0.015
Weight (mg)	152.6 ± 1.65	155.3 ± 1.98	140.2 ± 1.74
% Moisture content	2.62 ± 0.97	1.58 ± 0.41	1.95 ± 0.72s
% Moisture uptake	1.31 ± 0.22	1.95 ± 0.43	1.25 ± 0.55
Tensile Strength (g/cm^2)	741.58 ± 15.93	1084.41 ± 19.06	702.00 ± 8.28
% Drug content	98.25 ± 1.25	99.12 ± 2.22	98.96 ± 2.03
Folding endurance	391 ± 4.72	409 ± 3.78	401 ± 4.93

* % w/w glycerol containing ATO loaded glycerosomal transdermal patch. (n=3, ± S.D.)

The results showed that increase in the moisture uptake was observed after addition of glycerosomes might be due to hygroscopic nature of glycerol present in glycerosomes [1]. The low moisture content and moisture uptake property of all patches indicated that it remained stable, avoiding brittleness and microbiological growth during storage [42]. The % drug content in all prepared patches was found to be greater than 95 % with uniform distribution of drug in patches. The folding endurance of prepared patch was found to be more than 350 indicating that the patch would retain its shape and integrity during application. The tensile strength of patch was increased after addition of glycerosomes might be due to plasticizer nature of glycerol which relaxes the hydrogen bonds that exist between polymers [41]. All prepared transdermal patches showed desired physicochemical characteristics and hence, were evaluated for further studies such as FTIR of treated skin, histopathology, fluorescence microscopic study and stability study.

9.15.1.2. RSNa loaded glycerosomal transdermal patch - Formulation development

The optimized RSNa loaded glycerosomes and liposomes (shown in chapter 6) were incorporated into above optimized transdermal patch and evaluated. The control transdermal patch was prepared by incorporating RSNa (in equivalent amount to RSNa loaded glycerosomes) instead of glycerosomes by using same method. The results are shown in table- 9.7.

Table- 9.7. Physicochemical characteristics of RSNa transdermal patches

PARAMETERS	VALUES		
	0 % w/w* (RLP)	30 % w/w* (RGP)	RSNa Loaded Patch (RTP)
Appearance	Clear and Translucent	Clear and Translucent	Clear and Transparent
Thickness (mm)	0.40 ± 0.005	0.42 ± 0.011	0.38 ± 0.015
Weight (mg)	154.8 ± 1.05	151.9 ± 0.95	139.2 ± 1.27
% Moisture content	2.41 ± 0.35	1.48 ± 0.45	1.74 ± 0.55
% Moisture uptake	1.89 ± 0.40	2.69 ± 0.55	1.21 ± 0.67
Tensile Strength (g/cm^2)	919.91 ± 16.23	1674.0 ± 11.53	878.08 ± 17.20
% Drug content	99.15 ± 1.52	99.03 ± 0.78	99.84 ± 1.42
Folding endurance	400 ± 2	415 ± 2	388 ± 4

*% w/w glycerol containing RSNa loaded glycerosomal transdermal patch. (n=3, ± S.D.)

From the obtained results, it was observed that all patches appeared transparent to translucent with smooth texture. There was no noticeable difference observed in their weight and thickness. The moisture content of prepared patches was observed in range of 1.48 to 2.41%. The results showed that moisture uptake was increased after the addition of glycerosomes, which might be due to the hygroscopic nature of glycerol, which absorbs water molecules. The folding endurance and tensile strength increased after addition of glycerosomes might be due to plasticizer nature of glycerol. The high folding endurance and tensile

strength indicates patch would retain its shape and integrity during application. All prepared patches showed desired physicochemical characteristics and were evaluated for further studies such as FTIR of treated skin, histopathology, fluorescence microscopic study, and stability study.

9.15.2. PECN incorporated transdermal patches:

Both ATO as well as RSNa PECN incorporated transdermal patch required addition of permeation enhancer to improve permeation of drug through skin layers. Hence, screening and optimization of permeation enhancer and its concentration was done for selection of optimum permeation enhancer and its concentration.

9.15.2.1. Screening and optimization of permeation enhancer:

The results of screening and optimization of permeation enhancers are shown in table- 9.8. Various permeation enhancers such as olive oil, glycerol, oleic acid, IPM and propylene glycol were screened and evaluated for drug skin permeation study and the permeation enhancer was optimized based on maximum amount of drug permeated through skin as shown in table-9.8.

Table- 9.8. Screening and optimization of permeation enhancer for drug-PECN transdermal patch

Permeation enhancer	% ATO skin permeation	% RSNa skin permeation
Olive oil	43.73 ± 1.52	37.38 ± 2.32
Oleic acid	47.22 ± 1.08	40.22 ± 1.56
Glycerol	**52.26 ± 2.53**	**47.11 ± 1.61**
Propylene glycol	46.86 ± 1.84	39.75 ± 1.86
IPM	41.67 ± 1.69	43.93 ± 1.09

(n=3, ± S.D.)

From the results, it was observed that the prepared ATO as well as RSNa-PECN transdermal patch containing glycerol (as permeation enhancer) showed maximum amount of drug permeated through skin layer as compared to other permeation enhancers. Hence, glycerol was selected as permeation enhancer in both ATO as well as RSNa loaded PECN transdermal patch for further studies.

9.15.2.2. Screening and optimization of concentration of permeation enhancer:

After selection of glycerol as permeation enhancer, its concentration was screened and optimized based on maximum % drug skin permeation. The % drug skin

permeation of prepared transdermal patch containing different concentration of glycerol are shown in table- 9.9.

Table- 9.9. Selection of concentration of permeation enhancer for drug-PECN transdermal patch

Concentration of permeation enhancer (%)	**% ATO skin permeation**	**% RSNa skin permeation**
0.1	46.82 ± 1.22	40.33 ± 1.83
0.2	**53.79 ± 2.59**	**48.85 ± 1.68**
0.3	54.44 ± 1.78	49.31 ± 1.98

(n=3, ± S.D.)

From the results, it was observed that 0.2 and 0.3 % w/w concentration of glycerol containing drug loaded PECN transdermal patch permeated more amount of drug through skin as compared to other concentration. It was observed that as the concentration of PE increases it results in increase in permeation of drug. There was no significant difference was observed for % drug permeation in 0.2 and 0.3 % glycerol concentration. Hence, 0.2 % w/w glycerol (PE) concentration was selected as optimum for preparation of both ATO as well as RSNa loaded PECN transdermal patch.

9.15.2.3. ATO-PECN transdermal patch - Formulation development

The optimised ATO-loaded PECN (shown in Chapter-7) was incorporated into the above-optimised patch and evaluated for physicochemical characteristics and other ex vivo studies. The control transdermal patch was prepared by incorporating ATO (in equivalent amount to ATO loaded PECN) instead of PECN by using same method.

The ATO incorporated transdermal patch and ATO-PECN incorporated transdermal patch with or without permeation enhancer with their physicochemical characteristics are shown in table- 9.10.

Table- 9.10. Physicochemical characteristics of ATO-PECN transdermal patches

PARAMETERS	VALUES		
	Without penetration enhancer* (AWTP)	**With Penetration enhancer* (APTP)**	**ATO Loaded transdermal Patch (ATP)**
Appearance	Clear and Transparent	Clear and Transparent	Clear and Transparent
Thickness (mm)	0.41 ± 0.005	0.44 ± 0.010	0.39 ± 0.005
Weight (mg)	150.2 ± 2.07	162.3 ± 1.81	144.6 ± 1.30
% Moisture content	2.36 ± 0.35	2.94 ± 0.33	1.84 ± 0.50
% Moisture uptake	1.20 ± 0.85	1.63 ± 0.61	1.58 ± 0.23
Tensile Strength (g/cm^2)	820.75 ± 11.67	1162.25 ± 19.55	766.25 ± 8.28
% Drug content	99.11 ± 1.08	98.26 ± 0.52	99.39 ± 0.66
Folding endurance	368 ± 4.04	399 ± 3.51	327 ± 3.61

*ATO loaded PECN (n=3, ± S.D.)

The prepared transdermal patches have transparent, uniform, smooth and flat surface which is essential criteria for suitable transdermal patches for application on skin. The drug content in all prepared batches was more than 95% showing homogenous drug distribution. The moisture uptake and moisture content of transdermal patch was found in the range of 0.58 ± 0.23 % to 1.63 ± 0.61 % and 1.84 ± 0.50 % to 3.36 ± 0.35 % respectively. The increased moisture uptake and moisture content after the addition of glycerol to the transdermal patch might be attributed to the hygroscopic nature of glycerol [1]. The low moisture uptake and moisture content indicates stability and resistance to microbial growth which is necessary to stay stable for long period of time and to reduce brittleness during storage [43, 44]. The folding endurance and tensile strength of ATO-PECN incorporated transdermal patch was increased as compared to ATO loaded transdermal patch might be due to formation of more complex three-dimensional structure of polymer with nanoparticles which provides mechanical strength to the

transdermal patch, thereby enhancing its folding endurance and tensile strength which prevents patch breakage. After addition of glycerol in ATO-PECN transdermal patch, folding endurance and tensile strength was increased might be due to plasticizer nature of glycerol which relaxes the intramolecular tension between polymer molecules helps to increase flexibility of transdermal patch [39, 45]. The patches showed high folding endurance indicating that they would not break and would maintain their integrity with general folding nature of skin when applied on skin [7, 43].

9.15.2.4. RSNa-PECN transdermal patch - Formulation development

The optimised RSNa-loaded PECN (shown in Chapter 8) was incorporated into the above-optimised patch and evaluated for physicochemical characteristics and other ex vivo studies. The control transdermal patch was prepared by incorporating RSNa (in equivalent amount to RSNa loaded PECN) instead of PECN by using same method. The RSNa-PECN incorporated transdermal patch required the addition of a permeation enhancer to improve the permeation of RSNa through skin layers and reach it to bloodstream. The screening and optimization of permeation enhancer and it's concentration for RSNa-PECN transdermal patch is shown in table- 9.8 and 9.9.

The RSNa incorporated transdermal patch and RSNa-PECN incorporated transdermal patch with or without permeation enhancer with their physicochemical characteristics is shown in table- 9.11.

Table- 9.11. Physicochemical characteristics of RSNa-PECN transdermal patches

PARAMETERS	VALUES		
	Without penetration enhancer* (RWTP)	**With Penetration enhancer* (RPTP)**	**RSNa Loaded transdermal Patch (RTP)**
Appearance	Clear and Transparent	Clear and Transparent	Clear and Transparent
Thickness (mm)	0.39 ± 0.004	0.43 ± 0.012	0.38 ± 0.004
Weight (mg)	153.3 ± 0.43	164.9 ± 0.46	148.3 ± 0.37
% Moisture content	3.45 ± 0.27	2.07 ± 0.13	1.82 ± 0.25
% Moisture uptake	1.53 ± 0.24	1.81 ± 0.28	1.87 ± 0.13
Tensile Strength (g/cm^2)	928.75 ± 20.30	1113.16 ± 13.50	813.08 ± 17.20
% Drug content	98.28 ± 0.5	98.65 ± 0.8	99.72 ± 1.0
Folding endurance	350 ± 3.68	372 ± 2.05	308 ± 2.49

(n=3, ± S.D.)

From the results, it was observed that all prepared patches showed desired physicochemical characteristics. All prepared patches showed high folding endurance and tensile strength with low moisture content as well as moisture uptake, indicating patches are stable and flexible.

9.16. Ex-vivo skin permeation study:

9.16.1. For ATO loaded glycerosomal transdermal patch:

The results of skin permeation study for glycerosomal patch (AGP), liposomal patch (ALP) and ATO incorporated patch (ATP) are shown in figure- 9.1 and table- 9.12. The results showed that more amount of ATO was permeated through skin by AGP as compared to ATP and ALP due to the elastic nature (deformable) of glycerosomes [29]. The results showed that the presence of glycerol significantly enhanced the permeation of ATO through the skin due to the fluidization of the stratum corneum and increased water content in the dense connective dermal layer, which promoted hydration and relaxation and facilitated the permeation of the drug [25, 46-48]. The amount of drug permeated through skin from ATP and ALP was found to be 52.06 and 63.07 % respectively, while 82.61% of drug permeated through skin from AGP. The average flux of ATP and ALP was found to be 17.31 and 21.71 µg/cm^2/hr respectively, while average flux for AGP was found to be 27.09 µg/cm^2/hr. The steady state flux of ATP and ALP was found to be 7.92 and 9.87 µg/cm^2/hr, while steady state flux for AGP was found to be 13.86 µg/cm^2/hr. The increased flux rate of glycerosomes might be attributed to glycerol's capacity to modify stratum corneum lipid organization and improve stratum corneum flexibility and hydration. The AGP enhanced drug permeation through skin by 1.24- and 1.56-fold as compared to ALP and ATP, respectively. In case of ATP, maximum amount of drug remained on the skin and minimum retention in the skin indicated that drug alone is unable to cross the skin barrier efficiently. Because the drug is lipophilic, permeation may have been complicated through the dermis, which is relatively hydrophilic. The drug skin retention and remained on skin was more in case of ALP as compared to AGP due to presence of deformable vesicles in AGP which facilitate permeation of vesicles through skin and avoid retention of drug into skin. On the basis of results, it was revealed that the glycerosomal transdermal patch has potential to permeate drug through skin layers.

Table- 9.12. *Ex vivo* skin permeation profile of ATP, ALP and AGP.

Time (In hrs)	ATP	ALP	AGP
0	0.00 ± 0.00	0.00 ± 0.00	0.00 ± 0.00
1	0.36 ± 0.19	0.27 ± 0.18	0.24 ± 0.11
2	3.29 ± 1.21	5.19 ± 1.25	3.73 ± 0.98
3	5.86 ± 0.97	7.39 ± 0.85	7.24 ± 1.24
4	7.61 ± 0.53	10.09 ± 1.69	10.69 ± 1.59
5	11.93 ± 1.96	12.29 ± 1.18	14.58 ± 1.74
6	12.68 ± 1.68	14.18 ± 1.91	18.33 ± 1.88
7	13.43 ± 1.88	16.19 ± 1.08	22.26 ± 1.49
8	14.33 ± 1.29	18.51 ± 0.63	27.69 ± 2.61
10	17.31 ± 1.63	23.00 ± 1.88	38.85 ± 1.87
12	20.12 ± 2.17	29.66 ± 1.56	51.24 ± 1.69
24	28.88 ± 2.09	38.11 ± 1.84	62.84 ± 2.47
30	35.71 ± 1.57	48.15 ± 2.76	68.44 ± 2.11
48	43.47 ± 1.69	53.67 ± 1.38	72.41 ± 1.63
72	52.06 ± 1.92	63.07 ± 1.52	82.61 ± 3.29
Parameters	**ATP**	**ALP**	**AGP**
Drug remained on skin (%)	41.91 ± 3.55	23.87 ±1.19	8.32 ± 1.07
Drug retained in skin (%)	9.36 ± 1.52	9.33 ± 0.69	4.16 ±1.11
Transdermal flux (J_{ss}) (μg/cm^2/hr)	17.31	21.71	27.09
Steady state flux	7.92	9.87	13.86
PER (As compared to ATP)**	1	1.24	1.56

** Permeation enhancement ratio (n=3, ±S.D.)

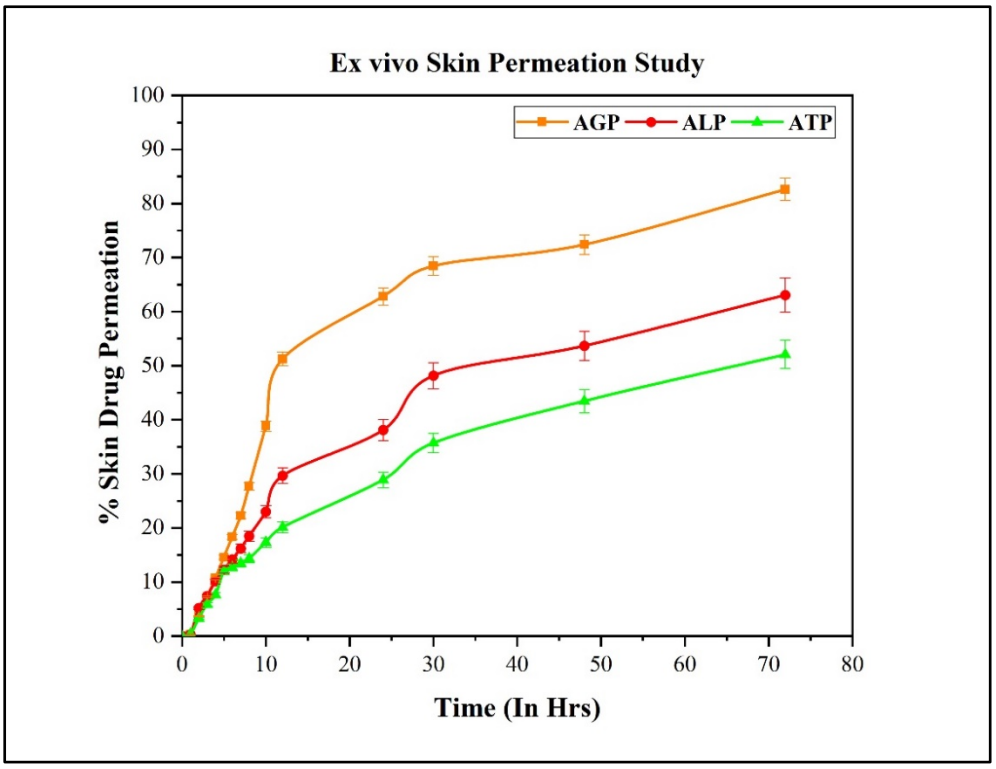

Figure- 9.1. Ex-vivo skin permeation profile of transdermal patches of ATP, ALP and AGP.

9.16.2. For RSNa loaded glycerosomal transdermal patch:

The results of skin permeation study for glycerosomal patch (RGP), liposomal patch (RLP) and RSNa incorporated patch (RTP) are shown in figure- 9.2 and table- 9.13. From the results, it was found that more amount of drug permeated through skin from RGP and RLP as compared to RTP. This happened due to nanosize of vesicles which facilitated the permeation of drug through skin. The RGP showed more permeation as compared RLP might be due to presence of glycerol containing vesicles which hydrates skin and loosens the dense connective tissue of dermis layer which facilitates the permeation of vesicles through skin layer [25]. The flexible (elastic) nature of glycerosomes present in RGP also facilitates permeation of drug to deep dermal layers [29]. The permeation enhancement ratio was found to be 1.67 and 2.36 for RLP and RGP as compared to RTP. The minimum skin retention and maximum drug remained on the skin in RTP, indicated that drug alone is unable to cross skin membrane due to highly hydrophilic nature of drug. The minimum skin retention and amount of drug remained skin was observed in RGP, due to the presence of glycerol containing vesicles which facilitates the permeation of drug

through skin due to deformable and elastic nature of vesicles. On the basis of results, we concluded that the glycerosomal transdermal patch is potential platform to permeate drug through skin.

Table- 9.13. *Ex vivo* skin permeation profile of RTP, RLP and RGP.

Time (In hrs)	RTP	RLP	RGP
0	0.00 ± 0.00	0.00 ± 0.00	0.00 ± 0.00
1	0.00 ± 0.00	0.12 ± 0.03	0.53 ± 0.39
2	0.44 ± 0.29	0.89 ± 0.21	1.92 ± 0.64
3	1.03 ± 0.50	2.25 ± 0.89	4.15 ± 1.23
4	2.22 ± 0.98	4.34 ± 1.04	6.65 ± 1.65
5	3.87 ± 1.22	6.12 ± 1.09	9.67 ± 1.87
6	4.64 ± 0.87	7.48 ± 1.61	15.66 ± 2.31
7	5.75 ± 1.54	9.32 ± 1.96	20.28 ± 2.09
8	6.59 ± 1.43	11.06 ± 1.20	24.25 ± 1.58
10	8.70 ± 1.99	14.41 ± 1.41	29.11 ± 1.65
12	10.41 ± 1.53	17.85 ± 1.98	35.41 ± 0.98
24	15.41 ± 1.69	24.84 ± 1.75	48.83 ± 2.61
30	19.68 ± 1.61	26.27 ± 1.42	54.36 ± 2.19
36	22.46 ± 1.03	31.96 ± 1.36	61.54 ± 1.57
48	26.46 ± 1.44	37.06 ± 1.21	74.41 ± 1.66
72	34.71 ± 2.97	48.77 ± 2.69	87.12 ± 3.04

Parameters	RTP	RLP	RGP
Drug remained on skin (%)	49.01 ± 1.82	28.28 ± 1.49	5.88 ± 1.20
Drug retained in skin (%)	14.24 ± 1.39	21.62 ± 1.77	8.37 ± 1.69
Transdermal flux (J_{ss}) (µg/cm^2/hr)	2.12	3.53	6.94
Steady state flux	1.93	2.69	5.00

PER (As compared to RTP)**	1	1.67	2.36

** Permeation enhancement ratio (n=3, ±S.D.)

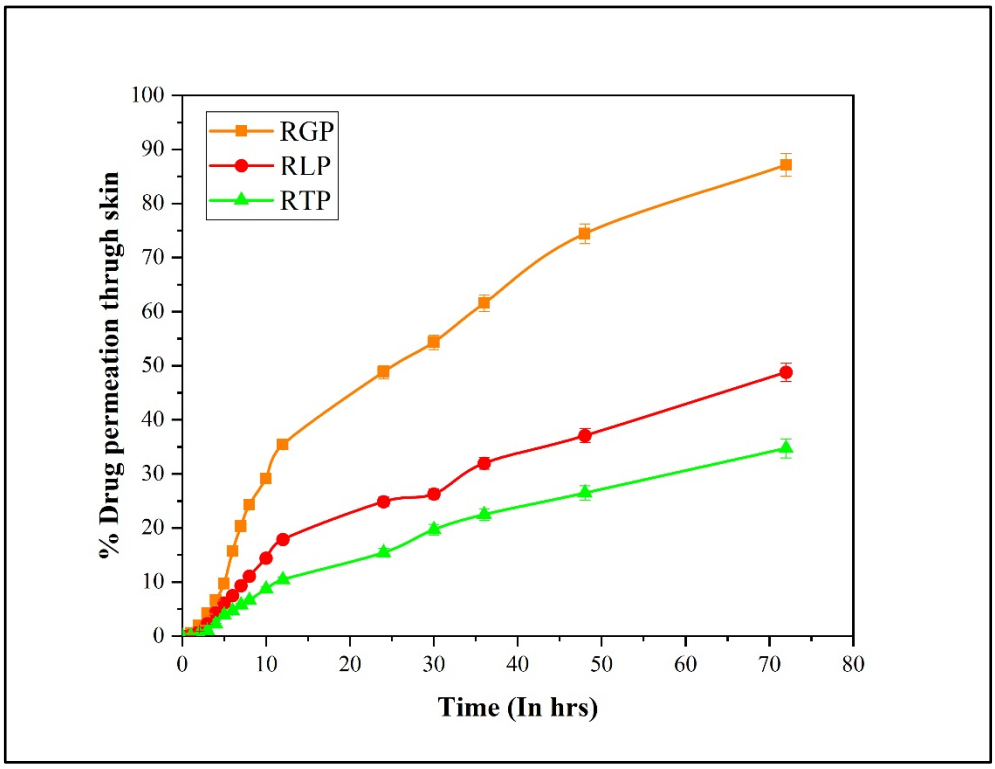

Figure- 9.2. Ex-vivo skin permeation profile of transdermal patches of RTP, RLP and RGP.

9.16.3. ATO-PECN transdermal patch:

The ex vivo skin permeation study of AWTP, APTP and ATP are shown in figure-9.3 and table- 9.14. The results showed that more amount of ATO was permeated through skin by APTP as compared to AWTP followed by ATP. APTP showed significant enhancement ($p<0.05$) in the permeation of ATO through skin layers. The % amount of drug permeated through skin from ATP and AWTP was found to be 48.73 ± 1.87 % and 68.02 ± 2.11 % respectively, while 83.22 ± 3.51% of drug permeated through skin from APTP. The AWTP showed more permeation of ATO through skin layer than ATP due to nanosize of biopolymeric particles and skin hydrating nature of chitosan [49] which helps to improve permeation of drug through skin. The average flux of ATP and AWTP was found to be 14.65 and 16.39 µg/cm^2/hr respectively, while average flux for APTP was found to be 24.09

µg/cm^2/hr. The steady state flux of ATP, AWTP and APTP was found to be 8.01, 11.07 and 13.54 µg/cm^2/hr. The APTP enhanced 1.22- and 1.70-folds drug permeation through skin as compared to AWTP and ATP respectively. The increase in drug permeation after the addition of glycerol may be due to hydration of the skin, which softens the keratin layer of stratum corneum, thereby increasing the diffusion of drug through skin [50-52]. In other words, the presence of glycerol enhances water activity on the upper side of the skin membrane, resulting in hydration and an increase in the proportion of fluid stratum corneum components, in addition to an increase in skin permeability [52]. Minimum skin deposition and higher drug remained on the skin were observed in AWTP as compared to APTP. This might be due to the presence of glycerol in APTP, which works synergistically with chitosan to hydrate the stratum corneum and help permeate the drug into the deep layers of the skin. In ATP, the maximum amount of drug remained on the skin, and the minimum retention in the skin indicated that drug alone is unable to cross the skin barrier efficiently. Due to the lipophilic nature of the drug, permeation may have been complicated through the dermis, which is relatively hydrophilic. On the basis of results, it was concluded that the APTP is a potential platform to permeate drug through the skin.

Table- 9.14. *Ex vivo* skin permeation profile of APTP, AWTP and APTP.

Time (In hrs)	ATP	AWTP	APTP
0	0.00 ± 0.00	0.00 ± 0.00	0.00 ± 0.00
1	0.09 ± 0.02	0.36 ± 0.11	0.44 ± 0.16
2	0.83 ± 0.23	1.89 ± 0.72	2.52 ± 1.20
3	1.99 ± 0.61	3.51 ± 0.51	5.94 ± 0.58
4	3.63 ± 1.32	5.85 ± 0.36	9.30 ± 1.36
5	5.69 ± 1.25	8.17 ± 1.59	11.97 ± 2.12
6	7.11 ± 0.93	10.85 ± 1.28	14.49 ± 1.85
7	9.17 ± 0.61	13.62 ± 1.64	21.47 ± 1.06
8	11.83 ± 1.39	16.31 ± 2.88	23.25 ± 1.58
10	14.54 ± 1.78	23.25 ± 1.52	32.26 ± 1.31
12	18.62 ± 1.06	30.39 ± 1.33	40.82 ± 2.39
24	28.58 ± 1.98	39.37 ± 1.89	56.93 ± 1.03
30	33.61 ± 1.11	42.51 ± 2.09	61.76 ± 1.98
48	41.36 ± 2.56	56.31 ± 1.48	70.25 ± 2.86
72	48.73 ± 1.63	65.02 ± 2.56	83.22 ± 3.67
Parameters	**ATP**	**AWTP***	**APTP***
Drug remained on skin (%)	39.85 ± 2.24	20.15 ± 1.58	8.42 ± 0.98
Drug retained in skin (%)	10.30 ± 1.01	8.42 ± 1.16	9.34 ± 1.08
Transdermal flux (J_{ss}) (µg/cm^2/hr)	14.65	16.39	24.09
Steady state flux	8.01	11.07	13.54
PER (As compared to ATP)**	1	1.22	1.70

*ATO-PECN incorporated transdermal patch (n=3, ±S.D.)

** Permeation enhancement ratio

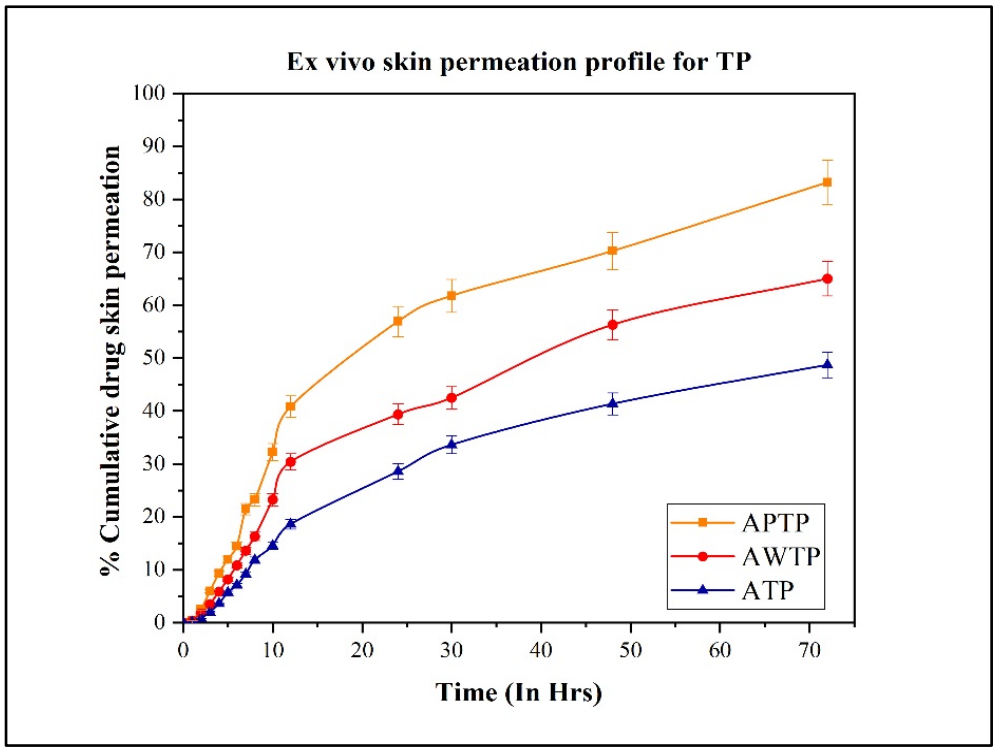

Figure- 9.3. Ex-vivo skin permeation profile of ATO transdermal patches

9.16.4. RSNa-PECN incorporated transdermal patch:

The ex vivo skin permeation study of RWTP, RPTP and RTP are shown in figure-9.4 and table-9.15. The results of ex vivo study showed that more amount of drug was permeated through skin from RWTP and RPTP as compared to RTP. The reason behind this behaviour is the presence of nanostructured PECN, which facilitates drug permeation through the skin. The RPTP showed more permeation of the drug as compared to the RWTP, which might be due to the hydrating nature of glycerol as well as chitosan [49], which helps to improve permeation of the drug through the skin. The PER for RPTP and RWTP was found to be 2.33 and 3.33 as compared to RSNa incorporated patch. The minimum amount of drug remained on the skin and was retained in the skin in the case of RPTP as compared to RWTP due to the presence of permeation enhancer, which synergistically helps to hydrate the skin layer and facilitate the permeation of drug through the skin. The maximum amount of drug that remained on the skin in RTP might be due to the hydrophilic nature of the drug, whose permeation is hindered by the lipophilic stratum corneum. On the basis of results, it was concluded that the RPTP is potential to permeate drug through skin.

Table- 9.15. *Ex vivo* skin permeation profile of RTP, RWTP and RPTP.

Time (In hrs)	RTP	RWTP*	RPTP*
0	0.00 ± 0.00	0.00 ± 0.00	0.00 ± 0.00
1	0.00 ± 0.00	0.55 ± 0.19	0.74 ± 0.21
2	0.00 ± 0.00	1.21 ± 0.62	3.21 ± 0.48
3	1.53 ± 0.25	3.51 ± 0.53	5.46 ± 1.00
4	2.89 ± 1.65	6.57 ± 1.52	8.53 ± 1.42
5	4.31 ± 0.76	9.06 ± 2.26	12.20 ± 1.68
6	5.09 ± 0.93	11.22 ± 1.20	15.42 ± 1.53
7	6.13 ± 0.82	14.65 ± 1.36	19.55 ± 1.87
8	7.55 ± 1.26	17.43 ± 1.98	23.74 ± 1.59
10	8.80 ± 1.54	21.31 ± 2.41	29.33 ± 0.99
12	10.96 ± 1.41	25.22 ± 1.27	37.51 ± 2.00
24	14.74 ± 0.63	31.46 ± 1.25	53.10 ± 1.59
30	20.87 ± 1.20	37.89 ± 1.63	60.96 ± 1.54
36	23.52 ± 1.60	43.89 ± 1.82	69.72 ± 1.87
48	27.34 ± 1.33	52.29 ± 1.44	77.66 ± 2.03
72	35.46 ± 1.71	69.83 ± 3.19	81.26 ± 2.57
Parameters	**RTP**	**RWTP***	**RPTP***
Drug remained on skin (%)	45.86 ± 1.68	13.66 ± 0.91	12.59 ± 1.22
Drug retained in skin (%)	17.15 ± 1.40	15.60 ± 1.12	4.77 ± 0.95
Transdermal flux (J_{ss}) (µg/cm^2/hr)	2.23	5.23	7.63
Steady state flux	1.95	3.70	5.03
PER (As compared to RTP)**	1	2.33	3.33

*RSNa-PECN transdermal patch (n=3, ±S.D.)

** Permeation enhancement ratio

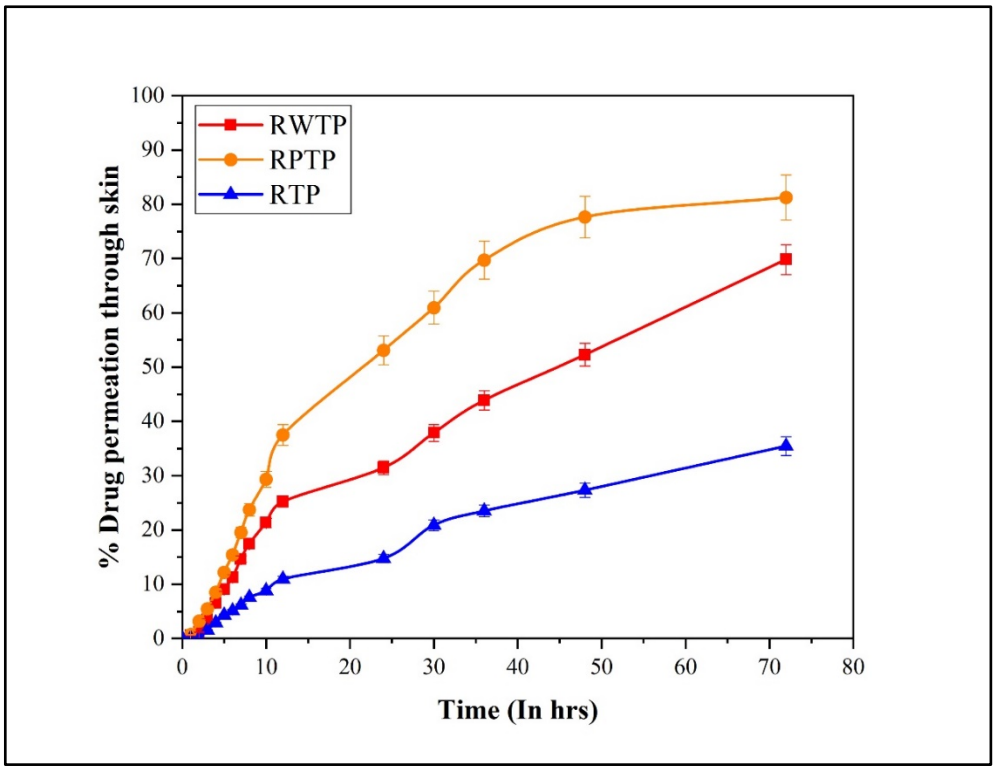

Figure- 9.4. Ex-vivo skin permeation profile of RSNa-PECN transdermal patches

9.17. Evaluation of skin structure integrity by FTIR-ATR study:

The effect of transdermal patch (containing drug loaded nanocarriers) on rat skin structure integrity after application was performed by FTIR-ATR as compared to normal skin. The FTIR spectra of all prepared transdermal patches are shown in figure- 9.5. Due to their molecular vibration, proteins and lipids in untreated skin produced various peaks in the FTIR spectrum. The untreated skin (normal skin) had characteristic peaks at 2852 cm^{-1} for asymmetric hydrocarbon, due to fatty acid and ceramide present in stratum corneum. The symmetric vibration of CH_2 in long-chain lipid hydrocarbons forms bands with wavenumbers of 2920 cm^{-1}. This compensates the lipid domain of the skin and is distinguished by its non-polar composition. The corneocytes and keratin have amide bond in the region of 1634 cm^{-1} and 1539 cm^{-1} are due to the C = O stretching vibrations of amide I and amide II respectively. The protein domain of skin is characterized by its polarity [25, 26, 48].

After treatment of glycerosomal transdermal patches, it was observed (figure- B and C) that slight increase in frequency of both polar and non-polar domain (blue shift) as compared non-treated skin (figure- A). This happened might be due to stratum corneum

or lipid layer fluidization and this, in turn, reduces the stratum corneum's barrier properties. Because of the presence of glycerol, the increased water content in the dense connective dermis layer induces hydration, loosens and thus facilitates diffusion of glycerosomal formulation through skin layer. This implies that glycerosomes improved skin penetration due to their ability to cause the hydration and lipid fluidization of skin layers [25, 46-48]. There was no other change in characteristic peaks of normal skin observed, which indicates excipients of glycerosomes loaded transdermal patch caused no harm to the skin integrity.

In FTIR spectra (figure- D and E) of PECN transdermal patch treated skin, blue shift was observed might be due to presence of glycerol as permeation enhancer which hydrates or fluidizes the stratum corneum. There was negligible variation in FTIR characteristic peaks of treated skin (figure- D and E) as compared to normal skin which confirmed that excipients of PECN loaded transdermal patch caused no harm to the skin integrity [26, 48, 53, 54].

From the overall results of FTIR study, it was concluded that all the prepared transdermal patches were safe to use.

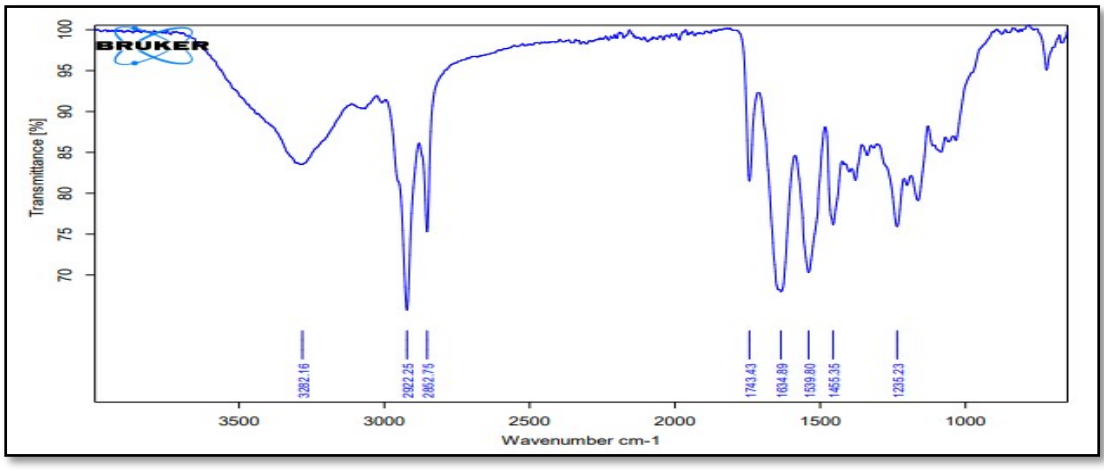

A. Non-treated skin

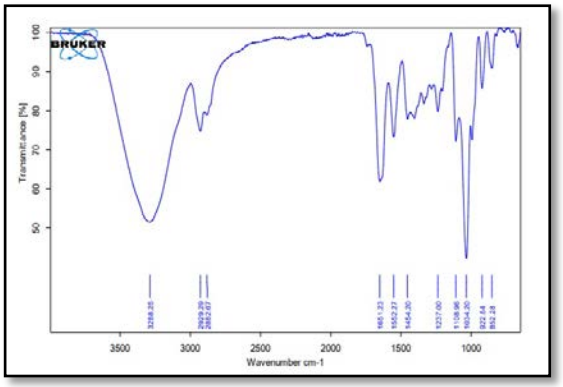

B. ATO loaded glycerosomal transdermal patch

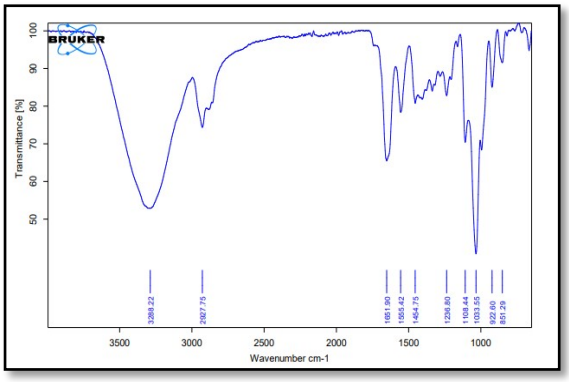

C. RSNa loaded glycerosomal transdermal patch

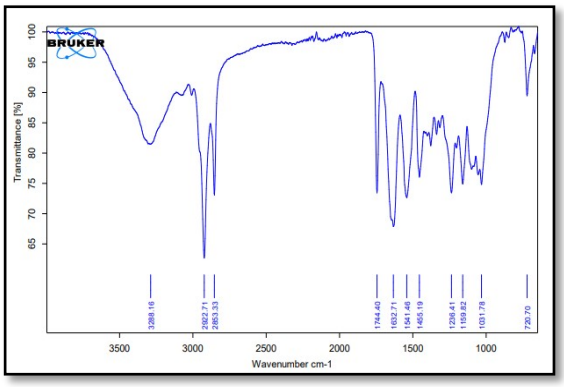

D. ATO-PECN incorporated transdermal patch

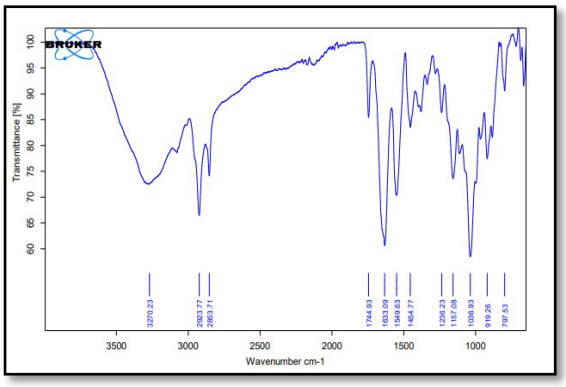

E. RSNa-PECN incorporated transdermal patch

Figure- 9.5. FTIR spectra of treated (B, C, D and E) and non-treated skin (A).

9.18. *Ex vivo* analysis of drug permeation through skin using fluorescence microscopy:

The fluorescence microscopic images of transdermal patch treated skin and untreated skin are shown in figure- 9.6 (a-d). The normal skin (non-treated) showed no fluorescence intensity, while skin treated with glycerosomal transdermal patches showed fluorescence intensity indicating the permeation of nanocarriers through skin layers. The intensity of fluorescence in skin layers was slightly more due to glycerosomes fuses with the skin lipids [25]. The more florescence intensity for glycerosomal transdermal patches might be due flexible nature of glycerosomes which make them highly deformable. The glycerosomes penetrates skin layers due to their ability to cross the cellular membrane efficiently. The overall results of fluorescence study conclude that the glycerosomal transdermal patches will be efficient to permeated drug through skin layers.

The results of fluorescence study for PECN incorporated transdermal patch showed higher fluorescence intensity than normal skin indicating that the PECN had ability to penetrate skin layers. The fluorescence intensity of treated skin (figure- C and D) compared with non-treated skin confirmed the proficient delivery of drug loaded PECN through skin with maintaining skin integrity [55].

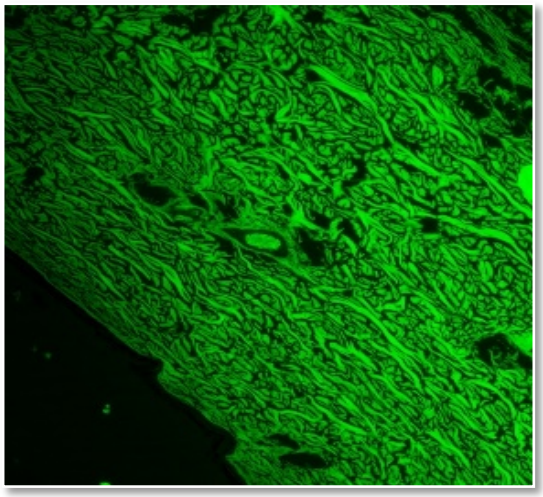

A. ATO loaded glycerosomal transdermal patch

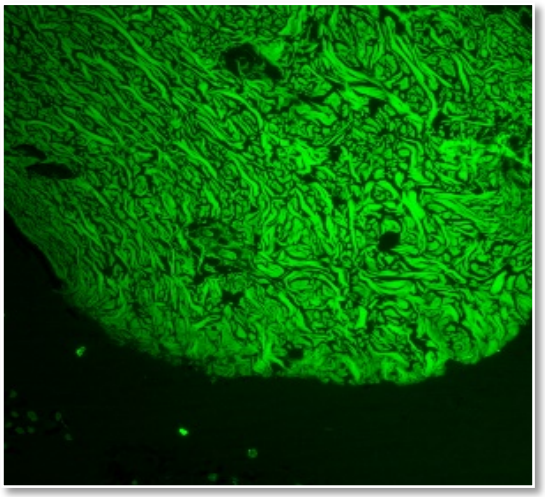

B. RSNa loaded glycerosomal transdermal patch

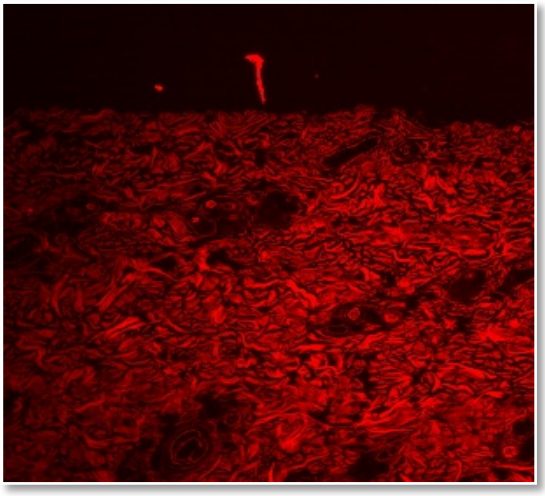

C. ATO-PECN loaded transdermal patch

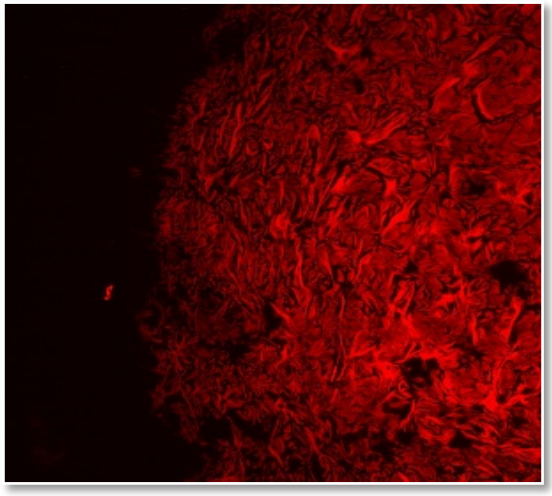

D. RSNa-PECN loaded transdermal patch

E. Non-treated skin

Figure- 9.6. Microscopic fluorescent images of treated (A, B, C and D) and non-treated skin (E)

9.19. Histopathology of Skin:

All skin samples were evaluated for any changes occurred in skin integrity. Histological analysis by H&E staining of normal skin and treated skin is shown in figure- 9.7 (A-F). The epidermal and dermal layers of normal skin were clearly visible in the photomicrographs (figure- 9.7B). It is feasible to see uniformly layered stratum corneum and loosely textured collagen in the dermis. The skin sample treated with isopropyl alcohol as a positive control showed considerable skin layer damage as a sign of toxicity and irritation (figure- 9.7A).

After treatment with nanocarriers incorporated transdermal patch, the upper stratum corneum layer of the treated skin showed minor disturbance but did not exhibit any change in the uniform arrangement of the dermis layer of the skin. According to the results, there was no change in skin integrity observed after treatment with a transdermal patch (figure- 9.7C – 9.7F).

According to the results of this histopathological investigation, the prepared transdermal patches are harmless and do not seem to cause skin damage.

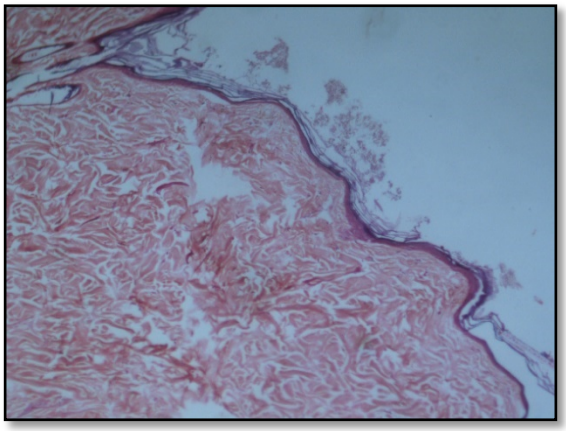

A. Treated with IPA

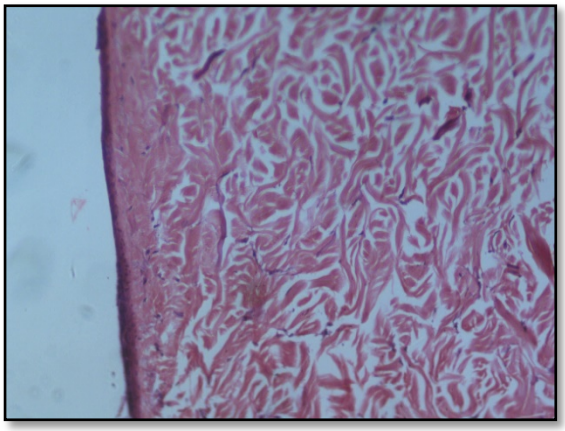

B. Untreated skin

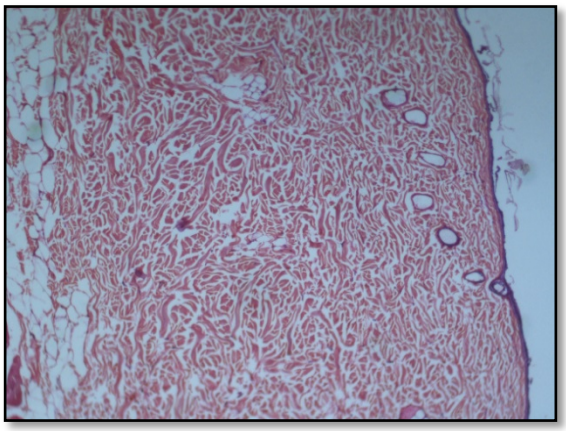

C. Treated with ATO loaded glycerosomal transdermal patch

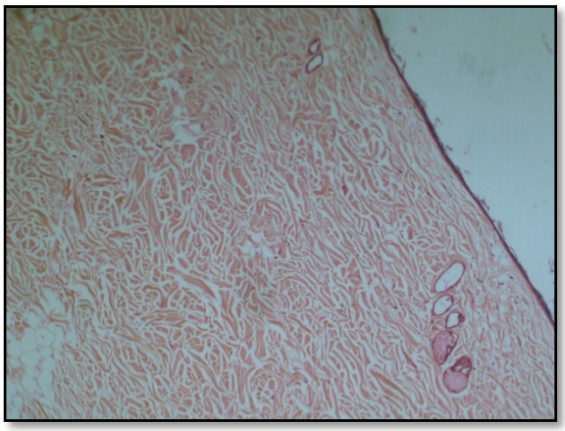

D. Treated with RSNa loaded glycerosomal transdermal patch

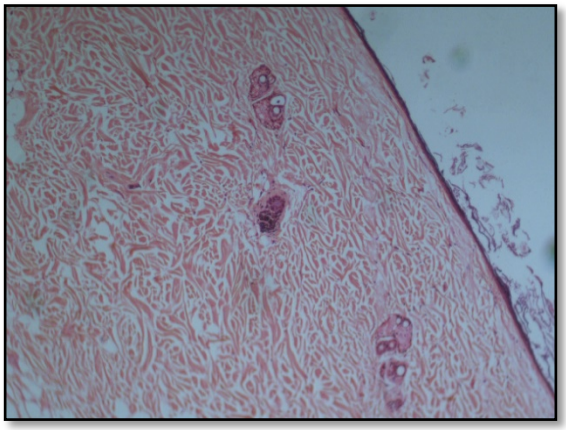

E. Treated with ATO-PECN loaded transdermal patch

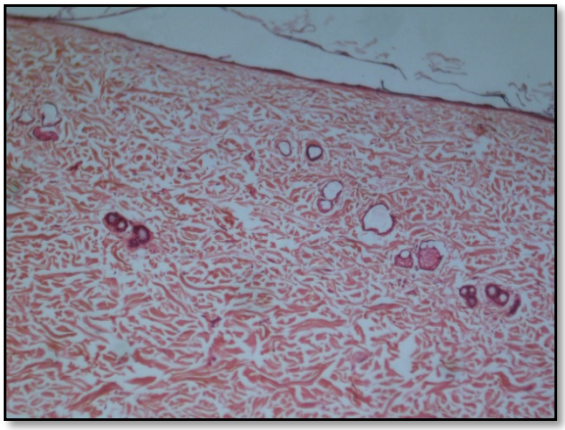

F. Treated with RSNa-PECN loaded transdermal patch

Figure- 9.7. Histopathological study of skin

9.20. Stability study:

The results of stability study for nanocarriers loaded transdermal patch are shown in figure- 9.8 (A-D). The results revealed that the 30 % w/w glycerol containing glycerosomal transdermal patch appeared clear, smooth, and translucent in nature after more than 90 days of stability and no significant difference was found in folding endurance, % drug content, weight, and thickness at 2-8°C and 25±2°C/60±5% RH conditions over for more than 90 days. But, slight increase in thickness and weight as well as decrease in folding endurance and % drug content was observed at 40±2°C/75±5% RH over 90 days. Thus, the drug loaded glycerosomal transdermal patch was stable at 2-8°C and 25±2°C/60±5% RH for more than 90 days. In case of liposomal transdermal patch, there was no noticeable change observed at 2-8°C for 90 days. There was slight difference observed at 25±2°C/60±5% RH and significant difference was observed in physicochemical parameters at 40±2°C/75±5% RH. On the basis of results, it was observed that glycerosomal transdermal patch more stable as compared to liposomal transdermal patch.

In the case of the PECN-incorporated transdermal patch, no significant differences were observed in folding endurance, appearance, weight, thickness, or percentage drug content at 2–8 °C and 25±2 °C/60±5% RH for more than 90 days. At 40±2 °C and 75±5% RH a slight increase in weight and thickness as well as a remark able decrease in folding endurance and % drug content were observed. Hence, it was concluded that the PECN incorporated transdermal patch was stable at 2-8°C and 25±2°C/60±5% RH over 90 days.

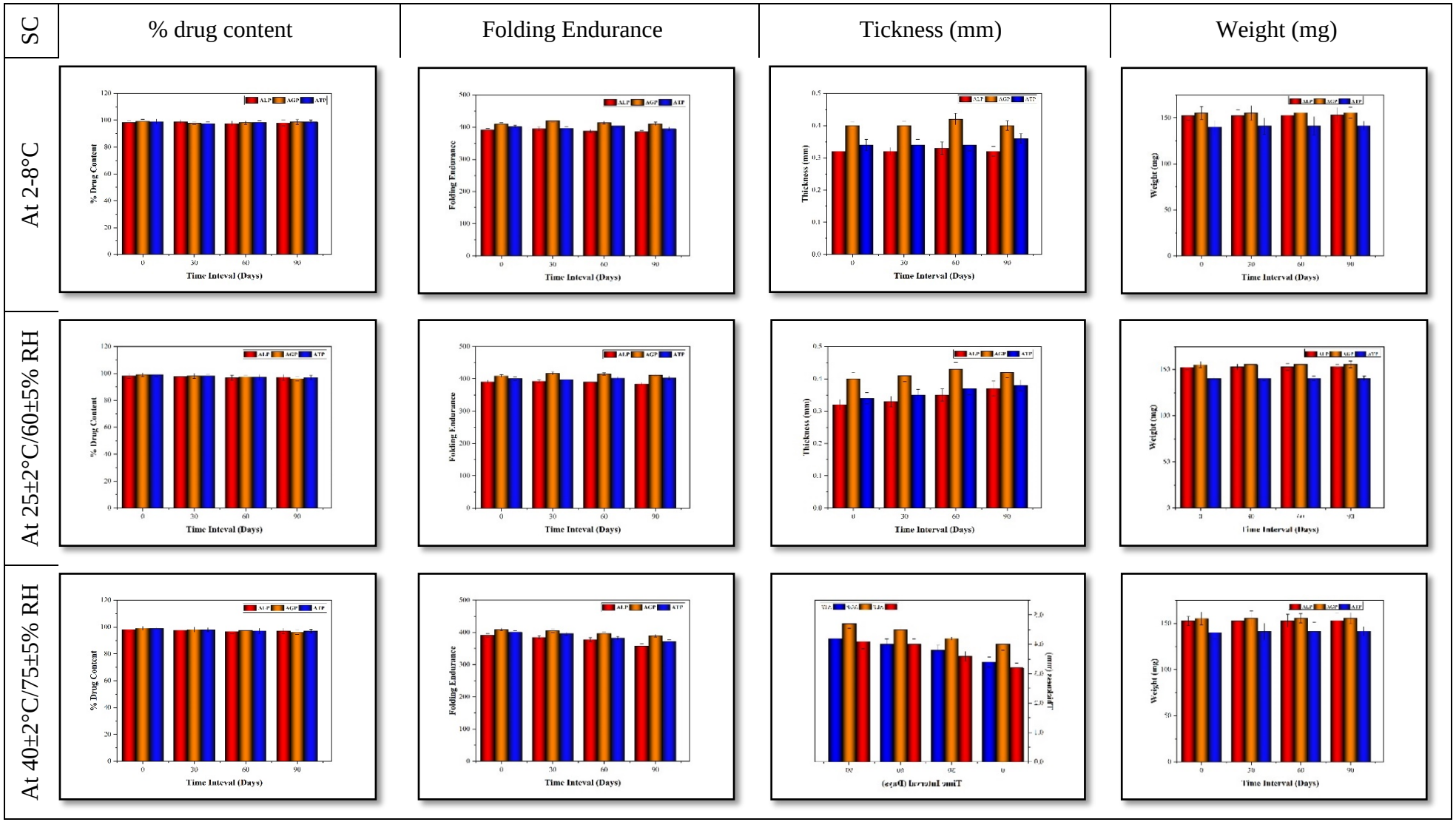

Figure- 9.8 (A). Stability study of ATO loaded glycerosomal transdermal patch

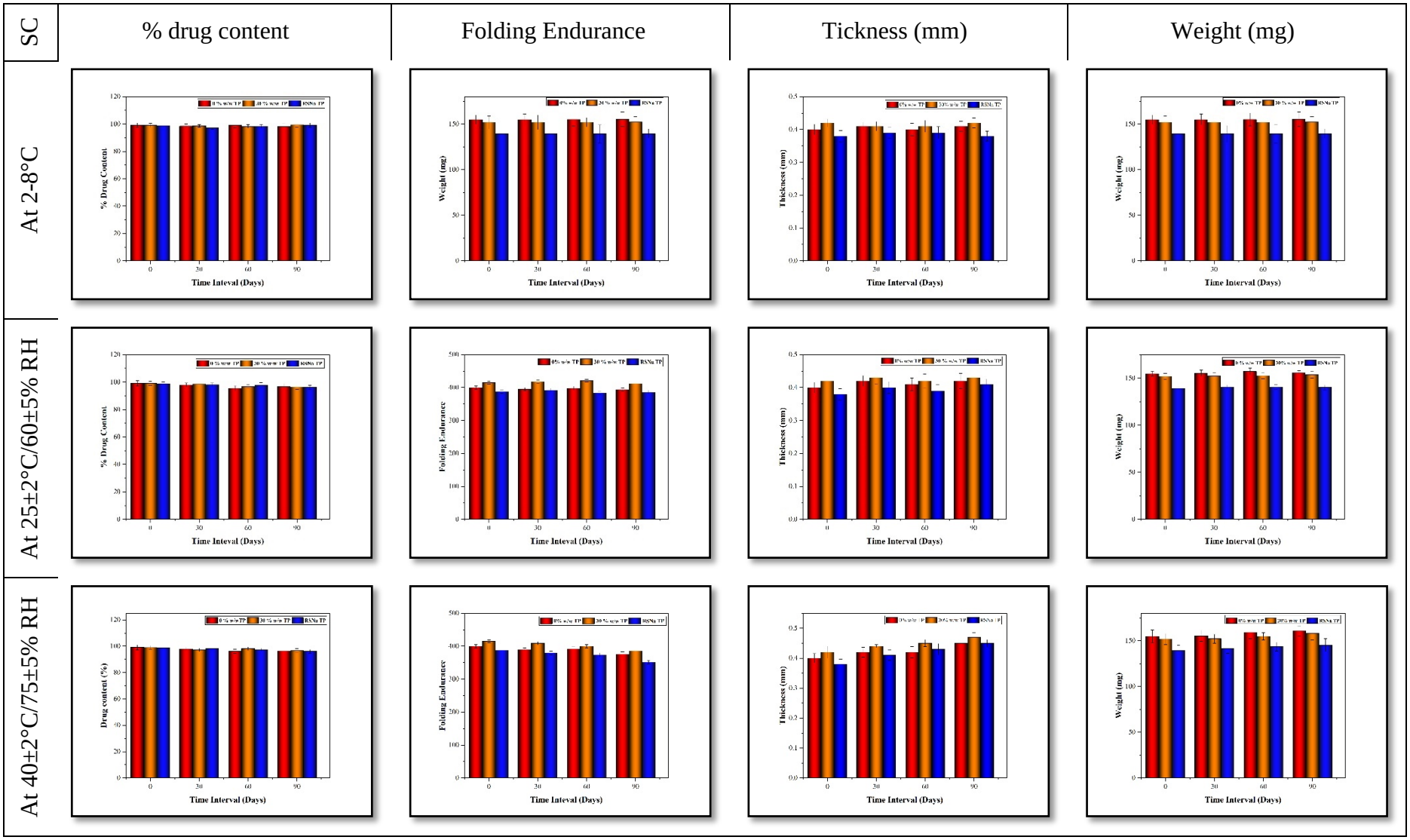

Figure- 9.8 (B). Stability study of RSNa loaded glycerosomal transdermal patch

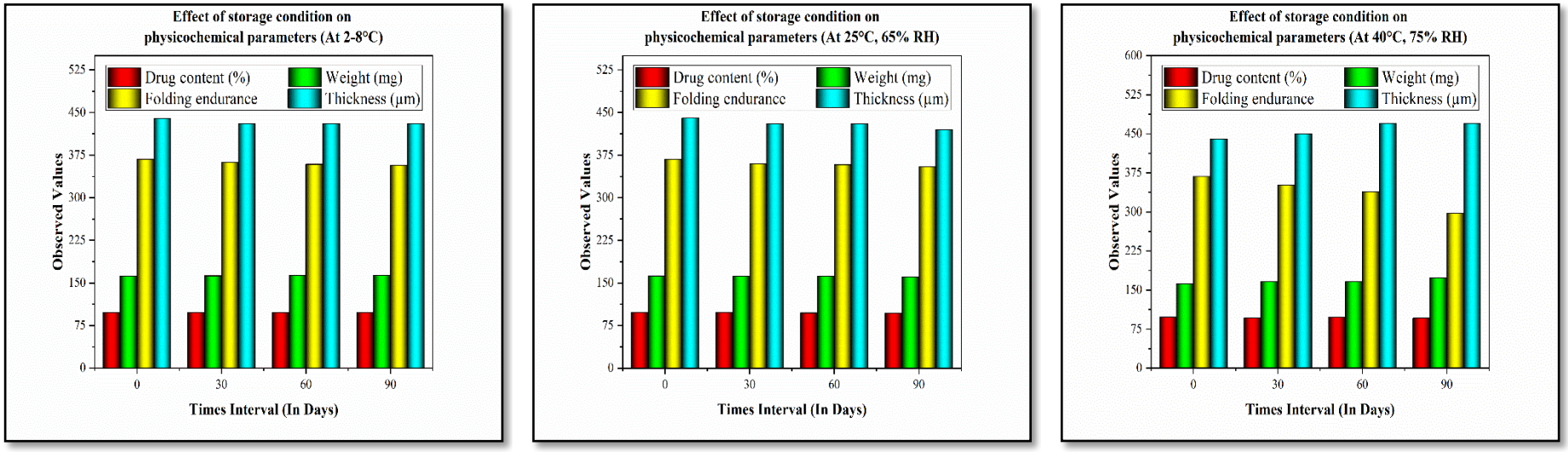

Figure- 9.8 (C). Stability study of ATO-PECN transdermal patch

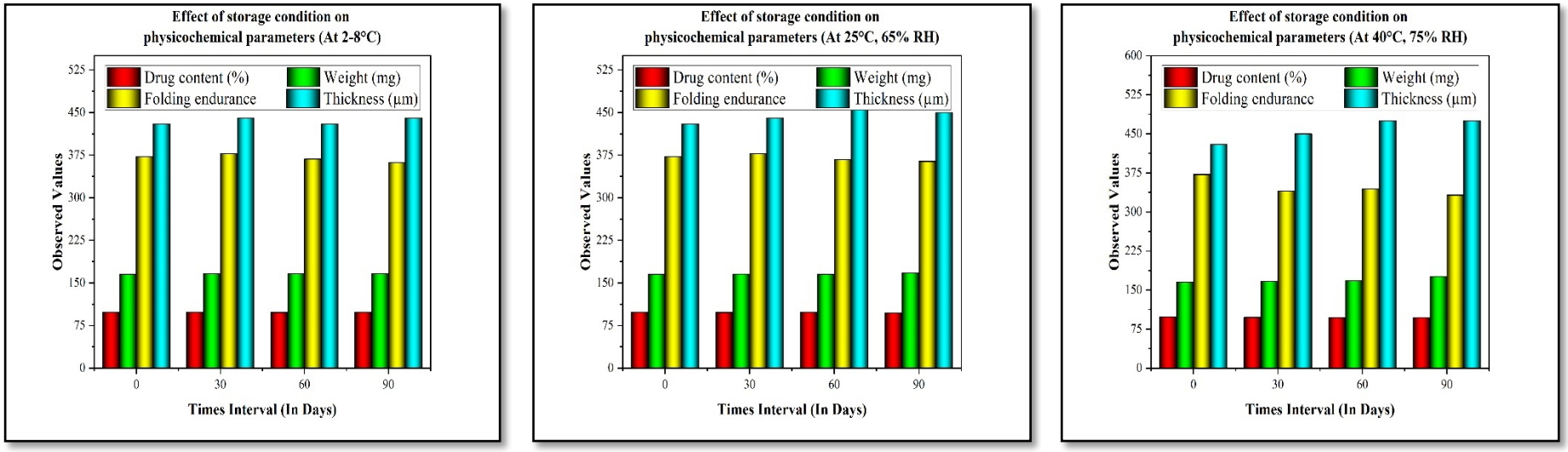

Figure- 9.8 (D). Stability study of RSNa-PECN transdermal patch

Chapter 9 – Nanocarriers incorporated transdermal patch

9.21. References:

1. Parhi, R. and T.J.J.o.p.i. Panchamukhi, *RSM-based design and optimization of transdermal film of ondansetron HCl.* Journal of Pharmaceutical Innovation, 2020. **15**: p. 94-109.

2. Agrawal, M.B., M.M.J.D.D. Patel, and I. Pharmacy, *Optimization and in vivo evaluation of quetiapine-loaded transdermal drug delivery system for the treatment of schizophrenia.* Drug Development and Industrial Pharmacy, 2020. **46**(11): p. 1819-1831.

3. Pastore, M.N., et al., *Transdermal patches: history, development and pharmacology.* British Journal of Pharmacology, 2015. **172**(9): p. 2179-2209.

4. Saroha, K., B. Yadav, and B.J.I.J.C.P.R. Sharma, *Transdermal patch: A discrete dosage form.* International Journal of Current Pharmaceutical Research, 2011. **3**(3): p. 98-108.

5. Alam, M.I., et al., *Type, preparation and evaluation of transdermal patch: A review.* WORLD JOURNAL OF PHARMACY AND PHARMACEUTICAL SCIENCES, 2013. **2**(4): p. 2199-2233.

6. Al Hanbali, O.A., et al., *Transdermal patches: Design and current approaches to painless drug delivery.* Acta Pharmaceutica, 2019. **69**(2): p. 197-215.

7. Nair, R.S., et al., *Matrix type transdermal patches of captopril: ex vivo permeation studies through excised rat skin.* Journal of Pharmacy Research, 2013. **6**(7): p. 774-779.

8. Verma, P. and S.S. Iyer, *Controlled Transdermal Delivery of Propranolol Using HPMC Matrices: Design and In-vitro and In-vivo Evaluation.* Journal of pharmacy and pharmacology, 2000. **52**(2): p. 151-156.

9. Malaiya, M.K., et al., *Controlled delivery of rivastigmine using transdermal patch for effective management of alzheimer's disease.* Journal of Drug Delivery Science and Technology, 2018. **45**: p. 408-414.

10. Singh, A., A.J.J.o.A.S. Bali, and Technology, *Formulation and characterization of transdermal patches for controlled delivery of duloxetine hydrochloride.* Journal of Analytical Science and Technology, 2016. **7**(1): p. 1-13.

11. Chandak, A.R. and P.R.P. Verma, *Development and evaluation of HPMC based matrices for transdermal patches of tramadol.* Clinical Research and Regulatory Affairs, 2008. **25**(1): p. 13-30.

12. Chandak, A.R., P.R.P.J.C.R. Verma, and R. Affairs, *Development and evaluation of HPMC based matrices for transdermal patches of tramadol.* Chem Cent J, 2008. **25**(1): p. 13-30.

13. Malaiya, M.K., et al., *Controlled delivery of rivastigmine using transdermal patch for effective management of alzheimer's disease.*

Journal of Drug Delivery Science and Technology, 2018. **45**: p. 408-414.

14. Akhlaq, M., et al., *Formulation and evaluation of anti-rheumatic dexibuprofen transdermal patches: a quality-by-design approach.* Taylor & Francis, 2016. **24**(7): p. 603-612.

15. Akhlaq, M., et al., *Formulation and evaluation of anti-rheumatic dexibuprofen transdermal patches: a quality-by-design approach.* Journal of drug targeting, 2016. **24**(7): p. 603-612.

16. Nair, R.S., et al., *Matrix type transdermal patches of captopril: ex vivo permeation studies through excised rat skin.* Journal of Pharmacy Research, 2013. **6**(7): p. 774-779.

17. Shende, P.K., et al., *Modulation of serratiopeptidase transdermal patch by lipid-based transfersomes.* Journal of Adhesion Science and Technology, 2015. **29**(23): p. 2622-2633.

18. Sarkar, G., et al., *Taro corms mucilage/HPMC based transdermal patch: An efficient device for delivery of diltiazem hydrochloride.* International Journal of Biological Macromolecules, 2014. **66**: p. 158-165.

19. Chauhan, M.K., P.K.J.C. Sharma, and p.o. lipids, *Optimization and characterization of rivastigmine nanolipid carrier loaded transdermal patches for the treatment of dementia.* Chemistry and Physics of Lipids, 2019. **224**: p. 104794.

20. Wavikar, P. and P.J.A.p. Vavia, *Nanolipidgel for enhanced skin deposition and improved antifungal activity.* AAPS PharmSciTech, 2013. **14**: p. 222-233.

21. Kim, H., et al., *Characteristics of skin deposition of itraconazole solubilized in cream formulation.* Pharmaceutics, 2019. **11**(4): p. 195.

22. Elshall, A.A., et al., *Ex vivo permeation parameters and skin deposition of melatonin-loaded microemulsion for treatment of alopecia.* Future Journal of Pharmaceutical Sciences volume, 2022. **8**(1): p. 28.

23. Chen, M., X. Liu, and A.J.I.j.o.p. Fahr, *Skin penetration and deposition of carboxyfluorescein and temoporfin from different lipid vesicular systems: In vitro study with finite and infinite dosage application.* International Journal of Pharmaceutics, 2011. **408**(1-2): p. 223-234.

24. Aboud, H.M., et al., *Development, optimization, and evaluation of carvedilol-loaded solid lipid nanoparticles for intranasal drug delivery.* AAPS pharmscitech, 2016. **17**(6): p. 1353-1365.

25. Moolakkadath, T., et al., *Preparation and optimization of fisetin loaded glycerol based soft nanovesicles by Box-Behnken design.* International Journal of Pharmaceutics, 2020. **578**: p. 119125.

26. Talib, S., et al., *Chitosan-chondroitin based artemether loaded nanoparticles for transdermal drug delivery system.* Journal of Drug Delivery Science and Technology, 2021. **61**: p. 102281.

27. Khan, D., et al., *Development of novel pH-sensitive nanoparticle-based transdermal patch for management of rheumatoid arthritis.* Nanomedicine, 2020. **15**(06): p. 603-624.

28. Gyanewali, S., et al., *Formulation development and in vitro–in vivo assessment of protransfersomal gel of anti-resorptive drug in osteoporosis treatment.* International Journal of Pharmaceutics, 2021. **608**: p. 121060.

29. Salem, H.F., et al., *Glycerosomal thermosensitive in situ gel of duloxetine HCl as a novel nanoplatform for rectal delivery: in vitro optimization and in vivo appraisal.* Drug Delivery and Translational Research volume, 2022. **12**(12): p. 3083-3103.

30. Nam, S.H., et al., *Topically administered Risedronate shows powerful anti-osteoporosis effect in ovariectomized mouse model.* Bone, 2012. **50**(1): p. 149-155.

31. Banerjee, S., et al., *Accelerated stability testing of a transdermal patch composed of eserine and pralidoxime chloride for prophylaxis against (±)-anatoxin A poisoning.* Journal of Food and Drug Analysis, 2014. **22**(2): p. 264-270.

32. Pichayakorn, W., et al., *Polymer blended deproteinized natural rubber reservoirs for nicotine transdermal patches: in vitro drug release, permeation study, and stability test.* Journal of Polymers and the Environment, 2022. **30**(3): p. 988-1000.

33. Parhi, R. and P.J.J.o.a.r. Suresh, *Transdermal delivery of Diltiazem HCl from matrix film: Effect of penetration enhancers and study of antihypertensive activity in rabbit model.* Journal of Advanced Research, 2016. **7**(3): p. 539-550.

34. Rao, M.R., et al., *Design of transdermal patch of ketoprofen by full factorial design for treatment of rheumatoid arthritis.* Journal of Drug Delivery and Therapeutics, 2019. **9**(2): p. 197-205.

35. Rajan, R., et al., *Design and in vitro evaluation of chlorpheniramine maleate from different eudragit based matrix patches: Effect of platicizer and chemical enhancers.* Ars Pharmaceutica 2010.

36. Parhi, R., P.J.M.S. Suresh, and E. C, *Formulation optimization and characterization of transdermal film of simvastatin by response surface methodology.* Materials Science and Engineering C, 2016. **58**: p. 331-341.

37. Rajabalaya, R.J.J.o.E. and F. Chemicals, *Studies on effect of plasticizer on invitro release and exvivo permeation from eudragit e100 based chlorpheniramine maleate*

matrix type transdermal delivery system. Journal of Excipients and Food Chemicals, 2010. **1**(2): p. 3-12.

38. Mishra, A. and A.J.C.R.i.P.S. Pathak, *Plasticizers: A vital excipient in novel pharmaceutical formulations.* Current Research in Pharmaceutical Sciences, 2017: p. 1-10.

39. Güngör, S., M.S. Erdal, and Y.J.R.a.i.p. Özsoy, *Plasticizers in transdermal drug delivery systems.* Recent Advances in Plasticizers, 2012. **5**: p. 91-112.

40. Gannu, R., et al., *Development of nitrendipine transdermal patches: in vitro and ex vivo characterization.* current drug delivery, 2007. **4**(1): p. 69-76.

41. Siddique, W., et al., *Impact of polymer and plasticizer on mechanical properties of film: A quality by design approach.* LATIN AMERICAN JOURNAL OF PHARMACY, 2021. **40**(12): p. 3002-3008.

42. Brito Raj, S., K.B. Chandrasekhar, and K.B.J.F.J.o.P.S. Reddy, *Formulation, in-vitro and in-vivo pharmacokinetic evaluation of simvastatin nanostructured lipid carrier loaded transdermal drug delivery system.* Future Journal of Pharmaceutical Sciences, 2019. **5**(1): p. 1-14.

43. Sarkar, G., et al., *Taro corms mucilage/HPMC based transdermal patch: An efficient device for delivery of diltiazem hydrochloride.* International journal of biological macromolecules, 2014. **66**: p. 158-165.

44. Chauhan, M.K. and P.K. Sharma, *Optimization and characterization of rivastigmine nanolipid carrier loaded transdermal patches for the treatment of dementia.* Chemistry and physics of lipids, 2019. **224**: p. 104794.

45. Ramadan, E., et al., *Design and in vivo pharmacokinetic study of a newly developed lamivudine transdermal patch.* Ars Pharmaceutica 2018. **4**(2): p. 166-174.

46. Bhattarai, N., et al., *PEG-grafted chitosan as an injectable thermosensitive hydrogel for sustained protein release.* Journal of Controlled Release, 2005. **103**(3): p. 609-624.

47. Boncheva, M., F. Damien, and V.J.B.e.B.A.-B. Normand, *Molecular organization of the lipid matrix in intact Stratum corneum using ATR-FTIR spectroscopy.* Biochimica et Biophysica Acta (BBA) - Biomembranes, 2008. **1778**(5): p. 1344-1355.

48. Obata, Y., et al., *Infrared spectroscopic study of lipid interaction in stratum corneum treated with transdermal absorption enhancers.* International Journal of Pharmaceutics, 2010. **389**(1-2): p. 18-23.

49. Gul, R., et al., *Biodegradable ingredient-based emulgel loaded with ketoprofen nanoparticles.* AAPS PharmSciTech, 2018. **19**: p. 1869-1881.

50. PRATAMA, F.N., et al., *The effect of glycerin as penetration enhancer in a ketoprofen solid preparation–patch on in vitro penetration study through rat skin.* 2020.

51. DAMGALI, Ş., et al., *Influence of Vehicles and Penetration Enhancers on the Permeation of Cinnarizine Through the Skin.* 2022. **19**(1): p. 19.

52. Björklund, S., et al., *Glycerol and urea can be used to increase skin permeability in reduced hydration conditions.* 2013. **50**(5): p. 638-645.

53. Dar, M.J., F.U. Din, and G.M. Khan, *Sodium stibogluconate loaded nano-deformable liposomes for topical treatment of leishmaniasis: macrophage as a target cell.* Drug delivery, 2018. **25**(1): p. 1595-1606.

54. Vaddi, H., et al., *Terpenes in ethanol: haloperidol permeation and partition through human skin and stratum corneum changes.* Journal of Controlled Release, 2002. **81**(1-2): p. 121-133.

55. Zsikó, S., et al., *Methods to Evaluate Skin Penetration In Vitro.* Scientia Pharmaceutica, 2019. **87**(3): p. 19.